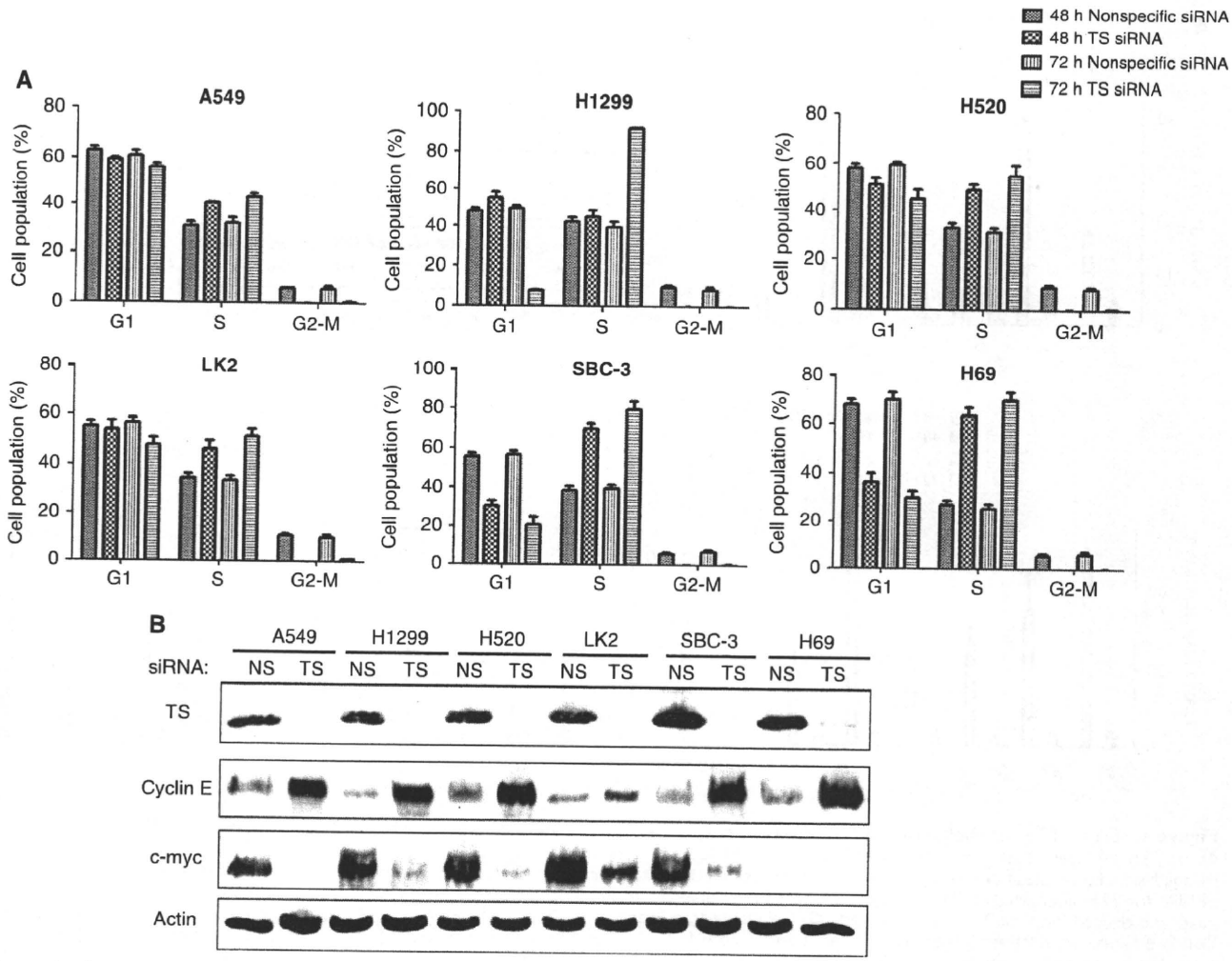

Figure 3 Effects of TS depletion on cell cycle distribution and on cyclin E and c-Myc expression in lung cancer cells. (**A**) The indicated cell lines were transfected with nonspecific (NS) or TS-1 siRNAs for 48 or 72 h and were then fixed, stained with propidium iodide, and analysed for cell cycle distribution by flow cytometry. Data are means ± s.d. of triplicates from experiments that were repeated on two additional occasions with similar results. (**B**) Cells were transfected with NS or TS-1 siRNAs for 72 h, after which cell lysates were prepared and subjected to immunoblot analysis with antibodies to TS, cyclin E, c-Myc, and β-actin. Transfection with the NS siRNA had no substantial effect on cell cycle distribution or on the expression of cyclin E or c-Myc compared with untreated cells.

modulated by mitochondrial proteins such as cytochrome *c*, Smac (also known as Diablo), and Omi (also known an HtrA2) (Hengartner, 2000; Srinivasula *et al*, 2003; Martinez-Ruiz *et al*, 2008). To investigate the mechanism of the downregulation of XIAP induced by TS depletion, we examined the release of these mitochondrial proteins into the cytosol. Immunoblot analysis revealed that the amounts of these mitochondrial proteins in the cytosol were increased by TS depletion in a time-dependent manner (Figure 5B). These data thus suggested that TS depletion-induced apoptosis is mediated, at least in part, by the mitochondrial signalling pathway.

DISCUSSION

Studies of TS-targeted therapy as well as the role of TS in DNA synthesis have provided the rationale for consideration of this enzyme as a prime therapeutic target. However, the precise mechanism by which inhibition of TS results in inhibition of tumour cell growth has remained incompletely understood. The aim of this study was therefore to investigate the underlying mechanism of the antiproliferative effect of specific TS inhibition in lung cancer cells with the use of an siRNA-based approach.

We first examined TS activity in lung cancer cell lines of different histotypes. Thymidylate synthase activity was determined with the use of the well-established 5-fluoro-dUMP binding assay. We found that TS activity was significantly higher in SCLC lines than in NSCLC lines, and that, among the latter, TS activity was higher in squamous cell carcinoma lines than in non-squamous cell carcinoma lines. A previous microarray analysis showed that mRNAs for proliferation-related proteins including TS were more abundant in SCLC lines than in NSCLC lines (Bhattacharjee *et al*, 2001). In addition, recent studies showed that the amount of TS mRNA was higher in resection specimens from patients with squamous cell carcinoma of the lung than in those from individuals with other histotypes of NSCLC (Ceppi *et al*, 2006; Ishihama *et al*, 2009; Monica *et al*, 2009). Given that TS activity in lung cancer cell lines was proportional to the abundance of TS protein in the present study (data not shown), our data showing a differential profile of TS activity among histotypes of lung cancer

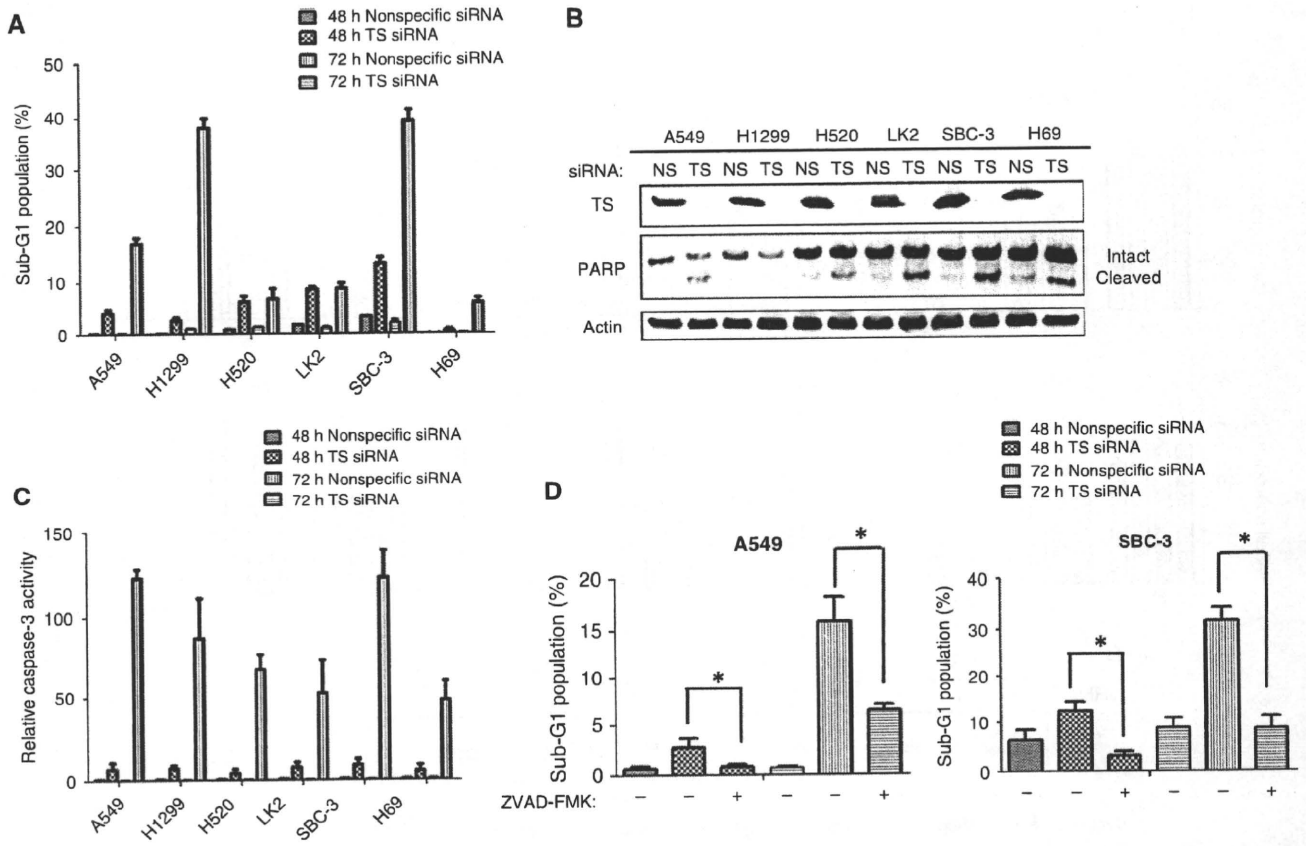

Figure 4 Effect of TS depletion on apoptosis in lung cancer cells. (**A**) The indicated cell lines were transfected with nonspecific (NS) or TS-1 siRNAs for 48 or 72 h and were then fixed, stained with propidium iodide, and subjected to flow cytometry for quantitation of the sub-G_1 population. Data are means ± s.d. of triplicates from experiments that were repeated on two additional occasions with similar results. (**B**) Cells were transfected with NS or TS-1 siRNAs for 72 h, after which cell lysates were prepared and subjected to immunoblot analysis with antibodies to TS, PARP, and β-actin. The positions of intact and cleaved forms of PARP are indicated. (**C**) Cells were transfected with NS or TS-1 siRNAs for 48 or 72 h, lysed, and assayed for caspase-3 activity. Data are expressed relative to the value for cells transfected with NS siRNA and are means ± s.d. from three independent experiments. (**D**) Cells were incubated for 2 h with or without ZVAD-FMK (50 μM), transfected with NS or TS-1 siRNAs for 48 or 72 h (in the continued absence or presence of ZVAD-FMK), and then evaluated for the size of the sub-G_1 population as in (**A**). Data are means ± s.d. of triplicates from experiments that were repeated on two additional occasions with similar results. *$P<0.05$ for the indicated comparisons. Transfection with the NS siRNA had no substantial effects on these markers of apoptosis compared with untreated cells.

are consistent with these previous findings. The cell line SCLC differs from NSCLC in terms of its faster growth and earlier spread (Allen and Jahanzeb, 2008), and recent clinical trials in NSCLC patients have revealed a poorer prognosis for squamous cell carcinoma than for adenocarcinoma (Asamura *et al*, 2008). The differential activity of TS among histotypes of lung cancer is thus suggestive of a role for this enzyme in promoting cell proliferation, with TS activity being a potential marker of tumour aggressiveness in lung cancer, although TS activity was not correlated with cell proliferation rate among the lung cancer cell lines examined in this study. We induced downregulation of both TS abundance and enzymatic activity in lung cancer cell lines by RNAi. The almost complete elimination of TS activity was associated with a marked antiproliferative effect in all tested lung cancer cell lines, including those with an original relatively low level of TS activity. These data suggest that TS is important for tumour cell proliferation in a manner independent of the original activity level.

We found that depletion of TS induced S-phase arrest and caspase-dependent apoptosis in lung cancer cells. Previous studies have shown that TS inhibition results in an imbalance between the amounts of dUTP and dTTP and a consequent decrease in the efficiency of DNA synthesis (Curtin *et al*, 1991; Houghton *et al*, 1993). Furthermore, this dUTP–dTTP imbalance results in misincorporation of dUTP into DNA and consequent DNA damage (Curtin *et al*, 1991; Houghton *et al*, 1993). In this study, we examined the effect of TS depletion on DNA damage as determined by immunofluorescence imaging of histone γ-H2AX foci, a sensitive and specific marker of DNA double-strand breaks (Burma *et al*, 2001; Stiff *et al*, 2004). Such foci were detected in ~90% of lung cancer cells transfected with TS siRNA (Supplementary Figure S1). Given that DNA damage or a reduced rate of DNA synthesis triggers the S-phase checkpoint mechanism (Sclafani and Holzen, 2007), the observed S-phase arrest induced by TS depletion likely results from activation of the S-phase checkpoint. Cellular responses to DNA damage are important for maintenance of genomic stability and cellular integrity (Bunz *et al*, 1998; Hirao *et al*, 2000). Cells either repair DNA damage or, if it is too severe for repair, initiate the cell death program (Zhao *et al*, 2001). Our data thus suggest that cells that arrest in S phase after TS depletion subsequently undergo apoptosis as a result of the accumulation of unrepairable DNA damage. We further showed that TS depletion resulted in upregulation of cyclin E and downregulation of c-Myc. Both cyclin E and c-Myc contribute to the transition of cells from G_1 to S phase (Wang *et al*, 2008; Malumbres and Barbacid, 2009) and have recently been implicated in promotion of caspase-dependent apoptosis subsequent to

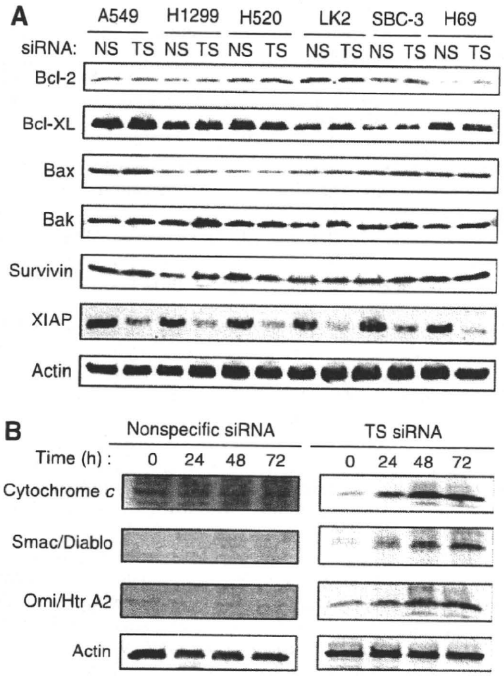

Figure 5 Effects of TS depletion on the expression of Bcl-2 and IAP family members and on the release of mitochondrial proteins into the cytosol in lung cancer cells. (**A**) The indicated cell lines were transfected with nonspecific (NS) or TS-1 siRNAs for 72 h, after which cell lysates were prepared and subjected to immunoblot analysis with antibodies to the indicated proteins. (**B**) SBC-3 cells were transfected with NS or TS-1 siRNAs for 24, 48, or 72 h, after which a cytosolic fraction was prepared and subjected to immunoblot analysis with antibodies to cytochrome *c*, Smac/Diablo, Omi/HtrA2, and *β*-actin. Transfection with the NS siRNA had no substantial effects on the abundance of Bcl-2 or IAP family proteins or on the release of mitochondrial proteins into the cytosol, compared with untreated cells.

S-phase arrest induced by DNA damage or inhibition of DNA synthesis in tumour cells (Mazumder *et al*, 2000; Leonce *et al*, 2001; Lu *et al*, 2009; Sankar *et al*, 2009). The effects of TS depletion on the abundance of cyclin E and c-Myc therefore likely contribute to the associated S-phase arrest and caspase-dependent apoptosis in lung cancer cells. Our present data thus suggest that the antiproliferative effect of TS depletion is attributable to S-phase arrest and the induction of caspase-dependent apoptosis in these cancer cells.

Our investigation of the mechanism by which TS depletion led to caspase-dependent apoptosis revealed that elimination of TS resulted in downregulation of XIAP, a member of the IAP family of proteins. Activation of the mitochondrial signalling pathway for apoptosis results in inhibition of IAP proteins and consequent promotion of caspase-dependent apoptosis (Hengartner, 2000; Takasawa *et al*, 2005; Yu *et al*, 2007). We also found that TS depletion resulted in the release of mitochondrial proteins, including cytochrome *c*, Smac/Diablo, and Omi/HtrA2, into the cytosol, suggestive of a link between activation of the mitochondrial pathway and downregulation of XIAP in lung cancer cells depleted of TS. Activation of the mitochondrial pathway is induced by a variety of stimuli including DNA damage (Hengartner, 2000). Given that TS depletion induced DNA double-strand breakage, our data suggest that loss of TS may contribute to activation of the mitochondrial pathway of apoptosis. We found that TS depletion did not affect the expression level of the IAP protein survivin. Further study will thus be needed to elucidate the precise mechanism by which XIAP is downregulated specifically in TS-depleted cells.

In conclusion, we have shown that the almost complete elimination of TS activity with an RNAi-based approach resulted in an apparently universal antiproliferative effect in lung cancer cells that was attributable to S-phase arrest and the induction of apoptosis. High levels of TS expression have been suggested to predict resistance to TS-targeted agents such as 5-fluorouracil (Johnston *et al*, 2003; Showalter *et al*, 2008). The new TS-targeted agent pemetrexed was found to have low activity in the treatment of SCLC (Ceppi *et al*, 2006; Socinski *et al*, 2009), possibly as a result of a high level of TS expression in such tumours. Our results now suggest that TS depletion inhibits the growth of lung cancer cells including SCLC cells with a high original activity of TS. This apparent discrepancy may be explained by the fact that 5-fluorouracil and pemetrexed inhibit TS activity by only ~60% (van Triest *et al*, 1997, 1999; Codacci-Pisanelli *et al*, 2002; Giovannetti *et al*, 2008), whereas our siRNA-based method inhibit TS activity almost completely. Our present results thus suggest that novel TS-targeted agents with an increased inhibitory efficacy might prove beneficial for the treatment of lung cancer regardless of histotype. They further provide a rationale for future clinical investigation of the therapeutic efficacy of TS-targeted agents for lung cancer patients.

Supplementary Information accompanies the paper on British Journal of Cancer website (http://www.nature.com/bjc)

REFERENCES

Allen J, Jahanzeb M (2008) Extensive-stage small-cell lung cancer: evolution of systemic therapy and future directions. *Clin Lung Cancer* **9:** 262–270

Asamura H, Goya T, Koshiishi Y, Sohara Y, Eguchi K, Mori M, Nakanishi Y, Tsuchiya R, Shimokata K, Inoue H, Nukiwa T, Miyaoka E (2008) A Japanese Lung Cancer Registry study: prognosis of 13,010 resected lung cancers. *J Thorac Oncol* **3:** 46–52

Bhattacharjee A, Richards WG, Staunton J, Li C, Monti S, Vasa P, Ladd C, Beheshti J, Bueno R, Gillette M, Loda M, Weber G, Mark EJ, Lander ES, Wong W, Johnson BE, Golub TR, Sugarbaker DJ, Meyerson M (2001) Classification of human lung carcinomas by mRNA expression profiling reveals distinct adenocarcinoma subclasses. *Proc Natl Acad Sci USA* **98:** 13790–13795

Bunz F, Dutriaux A, Lengauer C, Waldman T, Zhou S, Brown JP, Sedivy JM, Kinzler KW, Vogelstein B (1998) Requirement for p53 and p21 to sustain G2 arrest after DNA damage. *Science* **282:** 1497–1501

Burma S, Chen BP, Murphy M, Kurimasa A, Chen DJ (2001) ATM phosphorylates histone H2AX in response to DNA double-strand breaks. *J Biol Chem* **276:** 42462–42467

Carreras CW, Santi DV (1995) The catalytic mechanism and structure of thymidylate synthase. *Annu Rev Biochem* **64:** 721–762

Ceppi P, Volante M, Saviozzi S, Rapa I, Novello S, Cambieri A, Lo Iacono M, Cappia S, Papotti M, Scagliotti GV (2006) Squamous cell carcinoma of the lung compared with other histotypes shows higher messenger RNA and protein levels for thymidylate synthase. *Cancer* **107:** 1589–1596

Codacci-Pisanelli G, Van der Wilt CL, Smid K, Noordhuis P, Voorn D, Pinedo HM, Peters GJ (2002) High-dose 5-fluorouracil with uridine-diphosphoglucose rescue increases thymidylate synthase inhibition but not 5-fluorouracil incorporation into RNA in murine tumors. *Oncology* **62:** 363–370

Costi MP, Ferrari S, Venturelli A, Calo S, Tondi D, Barlocco D (2005) Thymidylate synthase structure, function and implication in drug discovery. *Curr Med Chem* **12:** 2241–2258

Curtin NJ, Harris AL, Aherne GW (1991) Mechanism of cell death following thymidylate synthase inhibition: 2′-deoxyuridine-5′-triphosphate accumulation, DNA damage, and growth inhibition following exposure to CB3717 and dipyridamole. *Cancer Res* **51:** 2346–2352

Ferguson PJ, Collins O, Dean NM, DeMoor J, Li CS, Vincent MD, Koropatnick J (1999) Antisense down-regulation of thymidylate synthase to suppress growth and enhance cytotoxicity of 5-FUdR, 5-FU and Tomudex in HeLa cells. *Br J Pharmacol* **127:** 1777–1786

Flynn J, Berg RW, Wong T, van Aken M, Vincent MD, Fukushima M, Koropatnick J (2006) Therapeutic potential of antisense oligodeoxynucleotides to down-regulate thymidylate synthase in mesothelioma. *Mol Cancer Ther* **5:** 1423–1433

Giovannetti E, Lemos C, Tekle C, Smid K, Nannizzi S, Rodriguez JA, Ricciardi S, Danesi R, Giaccone G, Peters GJ (2008) Molecular mechanisms underlying the synergistic interaction of erlotinib, an epidermal growth factor receptor tyrosine kinase inhibitor, with the multitargeted antifolate pemetrexed in non-small-cell lung cancer cells. *Mol Pharmacol* **73:** 1290–1300

Hengartner MO (2000) The biochemistry of apoptosis. *Nature* **407:** 770–776

Hirao A, Kong YY, Matsuoka S, Wakeham A, Ruland J, Yoshida H, Liu D, Elledge SJ, Mak TW (2000) DNA damage-induced activation of p53 by the checkpoint kinase Chk2. *Science* **287:** 1824–1827

Houghton JA, Morton CL, Adkins DA, Rahman A (1993) Locus of the interaction among 5-fluorouracil, leucovorin, and interferon-alpha 2a in colon carcinoma cells. *Cancer Res* **53:** 4243–4250

Ishihama H, Chida M, Araki O, Karube Y, Seki N, Tamura M, Umezu H, Honma K, Masawa N, Miyoshi S (2009) Comparison of 5-fluorouracil-related gene expression levels between adenocarcinomas and squamous cell carcinomas of the lung. *Jpn J Clin Oncol* **39:** 33–36

Johnston PG, Benson III AB, Catalano P, Rao MS, O'Dwyer PJ, Allegra CJ (2003) Thymidylate synthase protein expression in primary colorectal cancer: lack of correlation with outcome and response to fluorouracil in metastatic disease sites. *J Clin Oncol* **21:** 815–819

Koizumi F, Shimoyama T, Taguchi F, Saijo N, Nishio K (2005) Establishment of a human non-small cell lung cancer cell line resistant to gefitinib. *Int J Cancer* **116:** 36–44

Kubota K, Niho S, Enatsu S, Nambu Y, Nishiwaki Y, Saijo N, Fukuoka M (2009) Efficacy differences of pemetrexed by histology in pretreated patients with stage IIIB/IV non-small cell lung cancer: review of results from an open-label randomized phase II study. *J Thorac Oncol* **4:** 1530–1536

Leonce S, Perez V, Lambel S, Peyroulan D, Tillequin F, Michel S, Koch M, Pfeiffer B, Atassi G, Hickman JA, Pierre A (2001) Induction of cyclin E and inhibition of DNA synthesis by the novel acronycine derivative S23906-1 precede the irreversible arrest of tumor cells in S phase leading to apoptosis. *Mol Pharmacol* **60:** 1383–1391

Lin SB, Ts'o PO, Sun SK, Choo KB, Yang FY, Lim YP, Tsai HL, Au LC (2001) Inhibition of thymidylate synthase activity by antisense oligodeoxynucleotide and possible role in thymineless treatment. *Mol Pharmacol* **60:** 474–479

Lu X, Liu J, Legerski RJ (2009) Cyclin E is stabilized in response to replication fork barriers leading to prolonged S phase arrest. *J Biol Chem* **51:** 35325–35337

Malumbres M, Barbacid M (2009) Cell cycle, CDKs and cancer: a changing paradigm. *Nat Rev Cancer* **9:** 153–166

Martinez-Ruiz G, Maldonado V, Ceballos-Cancino G, Grajeda JP, Melendez-Zajgla J (2008) Role of Smac/DIABLO in cancer progression. *J Exp Clin Cancer Res* **27:** 48

Mazumder S, Gong B, Almasan A (2000) Cyclin E induction by genotoxic stress leads to apoptosis of hematopoietic cells. *Oncogene* **19:** 2828–2835

Monica V, Scagliotti GV, Ceppi P, Righi L, Cambieri A, Lo Iacono M, Saviozzi S, Volante M, Novello S, Papotti M (2009) Differential thymidylate synthase expression in different variants of large-cell carcinoma of the lung. *Clin Cancer Res* **15:** 7547–7552

Oguri T, Achiwa H, Bessho Y, Muramatsu H, Maeda H, Niimi T, Sato S, Ueda R (2005) The role of thymidylate synthase and dihydropyrimidine dehydrogenase in resistance to 5-fluorouracil in human lung cancer cells. *Lung Cancer* **49:** 345–351

Ozasa H, Oguri T, Uemura T, Miyazaki M, Maeno K, Sato S, Ueda R (2009) Significance of thymidylate synthase for resistance to pemetrexed in lung cancer. *Cancer Sci* **10:** 161–166

Plummer III H, Catlett J, Leftwich J, Armstrong B, Carlson P, Huff T, Krystal G (1993) c-Myc expression correlates with suppression of c-kit protooncogene expression in small cell lung cancer cell lines. *Cancer Res* **53:** 4337–4342

Rahman L, Voeller D, Rahman M, Lipkowitz S, Allegra C, Barrett JC, Kaye FJ, Zajac-Kaye M (2004) Thymidylate synthase as an oncogene: a novel role for an essential DNA synthesis enzyme. *Cancer Cell* **5:** 341–351

Sankar N, Kadeppagari RK, Thimmapaya B (2009) c-Myc-induced aberrant DNA synthesis and activation of DNA damage response in p300 knockdown cells. *J Biol Chem* **284:** 15193–15205

Sclafani RA, Holzen TM (2007) Cell cycle regulation of DNA replication. *Annu Rev Genet* **41:** 237–280

Showalter SL, Showalter TN, Witkiewicz A, Havens R, Kennedy EP, Hucl T, Kern SE, Yeo CJ, Brody JR (2008) Evaluating the drug-target relationship between thymidylate synthase expression and tumor response to 5-fluorouracil. Is it time to move forward? *Cancer Biol Ther* **7:** 986–994

Socinski MA, Smit EF, Lorigan P, Konduri K, Reck M, Szczesna A, Blakely J, Serwatowski P, Karaseva NA, Ciuleanu T, Jassem J, Dediu M, Hong S, Visseren-Grul C, Hanauske AR, Obasaju CK, Guba SC, Thatcher N (2009) Phase III study of pemetrexed plus carboplatin compared with etoposide plus carboplatin in chemotherapy-naive patients with extensive-stage small-cell lung cancer. *J Clin Oncol* **27:** 4787–4792

Spears CP, Gustavsson BG, Mitchell MS, Spicer D, Berne M, Bernstein L, Danenberg PV (1984) Thymidylate synthetase inhibition in malignant tumors and normal liver of patients given intravenous 5-fluorouracil. *Cancer Res* **44:** 4144–4150

Srinivasula SM, Gupta S, Datta P, Zhang Z, Hegde R, Cheong N, Fernandes-Alnemri T, Alnemri ES (2003) Inhibitor of apoptosis proteins are substrates for the mitochondrial serine protease Omi/HtrA2. *J Biol Chem* **278:** 31469–31472

Stiff T, O'Driscoll M, Rief N, Iwabuchi K, Lobrich M, Jeggo PA (2004) ATM and DNA-PK function redundantly to phosphorylate H2AX after exposure to ionizing radiation. *Cancer Res* **64:** 2390–2396

Takasawa R, Nakamura H, Mori T, Tanuma S (2005) Differential apoptotic pathways in human keratinocyte HaCaT cells exposed to UVB and UVC. *Apoptosis* **10:** 1121–1130

van Triest B, Pinedo HM, Telleman F, van der Wilt CL, Jansen G, Peters GJ (1997) Cross-resistance to antifolates in multidrug resistant cell lines with P-glycoprotein or multidrug resistance protein expression. *Biochem Pharmacol* **53:** 1855–1866

van Triest B, Pinedo HM, van Hensbergen Y, Smid K, Telleman F, Schoenmakers PS, van der Wilt CL, van Laar JA, Noordhuis P, Jansen G, Peters GJ (1999) Thymidylate synthase level as the main predictive parameter for sensitivity to 5-fluorouracil, but not for folate-based thymidylate synthase inhibitors, in 13 nonselected colon cancer cell lines. *Clin Cancer Res* **5:** 643–654

Wang H, Mannava S, Grachtchouk V, Zhuang D, Soengas MS, Gudkov AV, Prochownik EV, Nikiforov MA (2008) c-Myc depletion inhibits proliferation of human tumor cells at various stages of the cell cycle. *Oncogene* **27:** 1905–1915

Yu J, Wang P, Ming L, Wood MA, Zhang L (2007) SMAC/Diablo mediates the proapoptotic function of PUMA by regulating PUMA-induced mitochondrial events. *Oncogene* **26:** 4189–4198

Zhao H, Spitz MR, Tomlinson GE, Zhang H, Minna JD, Wu X (2001) Gamma-radiation-induced G2 delay, apoptosis, and p53 response as potential susceptibility markers for lung cancer. *Cancer Res* **61:** 7819–7824

Phase I and Pharmacologic Study of Weekly Bolus Topotecan for Advanced Non–Small-Cell Lung Cancer

Noriyuki Masuda,[1,2] Kaoru Matsui,[2] Shunichi Negoro,[3] Koji Takeda,[3] Shinzoh Kudoh,[4] Kazuhiko Nakagawa,[5] Akihira Mukaiyama,[6] Hiroaki Arase,[6] Pascal Yoshida,[6] Toshiyuki Ijima,[7] Minoru Takada,[2] Masahiro Fukuoka[5]

Abstract

Purpose: We conducted a phase I trial of the topoisomerase I inhibitor topotecan for the purpose of determining the maximum tolerated dose (MTD) and the dose-limiting toxicities (DLTs) of topotecan when administered weekly to patients with advanced non–small-cell lung cancer. **Patients and Methods:** Twelve patients with stage IIIB or IV disease were treated with topotecan by 30-minute intravenous infusion on days 1, 8, and 15 every 4 weeks. The dose was escalated in 2-mg/m^2 increments from the starting dose of 4 mg/m^2 until the MTD was reached. After the MTD had been reached in previously treated patients, chemotherapy-naive patients were enrolled for treatment at that dose, and the dose was escalated to estimate the MTD in the treatment-naive group. **Results:** The MTD of topotecan was determined to be 6 mg/m^2 in the previously treated group and 8 mg/m^2 in the chemotherapy-naive group. All 3 previously treated patients experienced DLT at the 6-mg/m^2 dose level. Although only 1 of the 3 previously treated patients experienced DLT (grade 4 neutropenia for ≥ 3 days) at the 8-mg/m^2 dose level, skipping the topotecan dose on day 15 because of neutropenia was reported in 2 patients. Anorexia and general fatigue were the common nonhematologic toxicities. **Conclusion:** The recommended dose of topotecan for phase II studies in previously untreated patients is 6 mg/m^2 on days 1, 8, and 15, every 28 days, and 4 mg/m^2 appears to be a suitable dose for use in previously treated patients with this schedule.

Clinical Lung Cancer, Vol. 11, No. 4, 271-279, 2010; DOI: 10.3816/CLC.2010.n.035
Keywords: Dose-limiting toxicity, Maximum tolerated dose, *N*-desmethyl topotecan, Pharmacokinetics

Introduction

Topotecan (Hycamtin; GlaxoSmithKline; Philadelphia, PA) is a water-soluble semisynthetic derivative of Camptothecin, a plant alkaloid extract from the Chinese tree *Camptotheca acuminata*.[1] Camptothecin is the only known potent inhibitor of DNA topoisomerase I.[2,3] Topotecan binds the DNA-topoisomerase I complex to form a stable noncleavable complex that blocks the progress of the replication fork, resulting in lethal damage during DNA replication and cell death.[4,5] Topotecan 1.5 mg/m^2 administered by intravenous (I.V.) infusion on days 1-5 of a 21-day cycle is approved single-agent treatment schedule. However, myelosuppression is dose limiting on this schedule in patients with small-cell lung cancer (SCLC), with approximately 70% of patients experiencing grade 4 neutropenia and 29% of patients developing grade 4 thrombocytopenia.[6] Furthermore, this standard regimen is not well tolerated by many elderly patients or by patients with comorbidities, poor performance status, or greater susceptibility to myelosuppression because of previous therapy. As a result, alternative dosing schedules have been explored to increase tolerability and convenience while optimizing antitumor activity; and one such schedule is administration of topotecan weekly. Moreover, topotecan is an S-phase–specific drug, and in vitro data obtained in non–small-cell lung cancer (NSCLC) cell lines showed that the cytotoxicity of topotecan was concentration dependent and

[1]Department of Respiratory Medicine, Kitasato University School of Medicine, 1-15-1 Kitasato Sagamihara Kanagawa, Japan
[2]Department of Thoracic Malignancy, Medical Center for Respiratory and Allergic Diseases of Osaka Prefecture, Osaka, Japan
[3]Department of Clinical Oncology, Osaka City General Hospital, Osaka, Japan
[4]Department of Respiratory Medicine, Osaka City Medical School, Osaka, Japan
[5]Department of Medical Oncology, Kinki University School of Medicine, Osaka, Japan
[6]Department & Medical Affairs Division, GlaxoSmithKline K.K., Tokyo, Japan
[7]Pharmaceuticals Marketing Division, Nippon Kayaku Co., Ltd., Tokyo, Japan

Submitted: Dec 17, 2009; Revised: Jan 27, 2010; Accepted: Feb 16, 2010

Address for correspondence: Noriyuki Masuda, MD, PhD, Department of Respiratory Medicine, Kitasato University School of Medicine, 1-15-1 Kitasato Sagamihara, Kanagawa, Japan
Fax: 81-42-778-8805; e-mail: masuda@med.kitasato-u.ac.jp

exposure-time dependent during the first 8-24 hours of exposure, after which the cells became less sensitive.[7] This resistance correlated with downregulation of topoisomerase I, and the topoisomerase I level returned to its baseline level 7 days after removing topotecan. The transient, reversible change in topoisomerase I supports the concept of weekly dosing of topotecan rather than the standard 5-day regimen. Weekly schedules of topotecan have been assessed in an attempt to increase tolerability and convenience in comparison with the standard 5-day regimen while at the same time optimizing antitumor activity. Furthermore, there is increasing evidence that weekly bolus infusions of topotecan are especially active against recurrent ovarian cancer[8-15] and cervical cancer.[16,17] However, the pharmacokinetics of topotecan when administered as a weekly infusion have not been established.

The objectives of this phase I study were (a) to determine the maximum tolerated dose (MTD), dose-limiting toxicity (DLT), and recommended dose of topotecan on the weekly bolus schedule; (b) to describe and quantify the clinical toxicities of topotecan on the weekly schedule; (c) to determine the pharmacokinetics of topotecan and whether there is a relationship between the pharmacokinetic parameters and clinical toxicities; and (d) to obtain preliminary evidence of therapeutic activity in patients with advanced NSCLC.

Patients and Methods

Patient Selection

Patients who met the following criteria were enrolled in this study: a histologic or cytologic diagnosis of stage IV NSCLC or stage III disease that was not a candidate for curative radiation therapy; no therapy within 4 weeks before entry (within 6 weeks for nitrosourea or mitomycin C); a measurable or evaluable lesion; a performance status of 0 or 1 on the Eastern Cooperative Oncology Group scale; a life expectancy of at least 3 months; adequate bone marrow function (leukocyte count, 4000-12,000/μL; neutrophil count ≥ 2000/μL; platelet count, ≥ 100,000/μL; and hemoglobin concentration, ≥ 9.5 g/dL), normal hepatic function (bilirubin, ≤ 1.5 mg/dL; aspartate aminotransferase and alanine aminotransferase levels ≤ 2.5 × the upper limit of normal [ULN]), and normal renal function (creatinine, ≤ the ULN and creatinine clearance ≥ 50 mL/min; aged between 20 and 74 years; and gave written informed consent to participation in the study obtained. After determination of the MTD for pretreated patients, no previous chemotherapy was allowed. Patients were ineligible if they had a serious infectious disease or any other serious complication (eg, heart disease, interstitial pneumonia, or uncontrollable diabetes); gastrointestinal bleeding or paralytic ileus; massive pleural or pericardial effusion, or ascites; symptomatic brain metastases; an active concurrent malignancy; were lactating or pregnant, or might become pregnant; unwilling to use contraception (for men); had a history of bone marrow transplantation; had a history of drug allergy; had been treated with topotecan; or had any other severe medical problem that might compromise compliance with the protocol. The study was approved in advance by the Institutional Review Board and by the Hospital Ethics Committee.

Drug Administration

Topotecan (SmithKline Beecham Pharmaceutical Co. Ltd.; Philadelphia, PA) is a lyophilized light-yellow powder containing 4 mg of active drug. The appropriate amount of topotecan was diluted in 100 mL of normal saline and administered intravenously as a 30-minute infusion on days 1, 8, and 15 every 28 days. The starting dose of topotecan was 4 mg/m^2 on this weekly schedule. The topotecan dose on days 8 and 15 was withheld if the leukocyte count was < 2000/μL, the neutrophil count < 1000/μL, or platelet count < 50, 000/μL.

Dosage and Dose Escalation Procedure

The study was designed to escalate the dose of topotecan by increments of 2 mg/m^2 in successive patient cohorts until the MTD was reached. Following the attainment of the MTD in patients with previous chemotherapy, the same dose escalation was carried out in patients with no previous chemotherapy from the MTD for pretreated patients. The DLT was defined as an absolute neutrophil count (ANC) < 500/μL or leukocyte count < 1000/μL for ≥ 3 days; febrile neutropenia (fever > 38.5°C with ANC < 1000/μL); platelet count < 20,000/μL; and nonhematologic toxicity (except nausea, vomiting, anorexia, fatigue, or alopecia) grade 3. At least 3 patients were to be included at each dose level. Escalation to the next dose level was allowed if none of the 3 patients developed DLT during the first cycle of treatment. If 1 of the 3 patients developed DLT, the number of patients at that level was expanded to 6 patients, and if fewer than 2 of the 6 patients experienced DLT, further dose escalation was allowed. If 2 or more of the 6 patients experienced DLT, that dose was concluded to be the MTD, and the next lower dose level would be recommended for use in further studies. No intrapatient dose escalation was allowed in this study.

The dose on days 8 and 15 was to be given only after confirming that the blood cell counts were within the reference levels (white blood cell [WBC] count ≥ 2000/μL; neutrophil count ≥ 1000/μL, platelet count ≥ 50,000/μL). If any of these levels were not met, the dose on that day was skipped.

Even if the dose on day 8 or 15 was skipped, the next course could be given if an antitumor effect was expected; however, the dose in the next course needed to be administered based on the criteria described below. The second and subsequent courses could be given unless an apparent increase in tumor size (progressive disease; PD) was observed in the previous course. In the treatment at the recommended dose, at least 2 courses were to be given to all patients except patients with PD. As a rule, the same dose as in the first course was given in the second and subsequent courses, starting 13 days after the final dose in the previous course, but only after confirming that the WBC count was ≥ 4000/μL, neutrophil count 2000/μL, platelet count ≥ 100,000/μL, and that the hemoglobin concentration showed a tendency to recover or was ≥ 9.5 g/dL.

When grade 4 leukopenia or neutropenia persisted for at least 3 days, or ≥ grade 3 neutropenia associated with a fever of ≥ 38.5°C or thrombocytopenia (< 20,000/μL) occurred in the previous course, the dose in the next course was reduced by 2 mg/m^2/day. When the dose on day 8 or 15 was skipped because of a low blood count below the reference level in the previous course, the dose in the next course was to be reduced by 2 mg/m^2/day.

Evaluation

Tumors were staged based on a complete medical history and the results of a physical examination, routine chest radiography, bone scintiscanning, computed tomography (CT) of the chest and

Table 1 Patient Characteristics

Characteristic	Number of Patients
Total Number of Patients	12
Sex	
Male	9
Female	3
Median Age, Years (Range)	63 (53-68)
Performance Status (ECOG)	
0	0
1	12
Previous Treatment	
Chemotherapy	2
Chemotherapy + radiation therapy	2
Chemotherapy + radiation therapy + surgery	2
None	6
Median Number of Previous Chemotherapy Regimens (Range)	0-1
Stage	
IIIB	4
IV	8
Histologic Diagnosis	
Adenocarcinoma	6
Squamous cell carcinoma	6

Abbreviation: ECOG = Eastern Cooperative Oncology Group

abdomen, whole-brain magnetic resonance imaging or CT scan, and fiberoptic bronchoscopy. Staging was performed according to the tumor-node-metastasis system.[18] Before the first course of treatment, a complete blood count (including a differential white cell count and platelet count); biochemistry tests (renal function, hepatic function, and electrolytes); electrocardiogram; and urinalysis were performed. The complete blood count and biochemistry tests were repeated at least twice a week after this initial evaluation, and the other examinations were repeated at least every 6 weeks to evaluate the target lesions. Adverse events were recorded and graded according to the National Cancer Institute Common Toxicity Criteria, Version 2.0. Tumor response was classified in accordance with the World Health Organization criteria.[19]

The duration of the response was recorded as the number of days from documentation of the response to the detection of disease progression.

Pharmacokinetics

A heparinized 2-mL blood sample for the pharmacokinetic study was obtained from the opposite arm of each patient before topotecan infusion and 0.5, 1, 2, 4, 8, 12, 24, and 48 hours (only for 8 mg/m^2) after the start of infusion on day 1 during the first treatment cycle. The blood was centrifuged immediately (3000 rpm for 15 minutes at 4°C), and 0.5 mL of the plasma obtained was placed in a tube containing 1 mL of cold methanol (–30°C). The mixture was vortexed and centrifuged (13,000*g* for 2 minutes at

Table 2 Dose-Limiting Toxicities During the First Cycle at Different Dose Levels

Variable	With Previous Therapy		No Previous Therapy	
	4 mg/m^2	6 mg/m^2	4 mg/m^2	6 mg/m^2
Number of Patients	3	3	3	3
Dose-Limiting Toxicity				
Febrile neutropenia (grade 4)	0	1	0	0
Infection (grade 4)	0	2	0	0
Grade 4 neutropenia ≥ 3 days	0	0	0	1
Number of patients who experienced DLT	0	3	0	1

Abbreviation: DLT = does-limiting toxicity

4°C), and the supernatant was stored at < –30°C until analyzed. A urine sample was collected before the initial dose was administered and from cumulative urine collected from 0 to 24 hours and from 24 to 48 hours after the first dose during the first cycle, and 10 mL aliquots were stored at < –30°C until analyzed. The plasma concentration of the lactone form of topotecan; the total plasma concentration of topotecan (sum of the lactone form and carboxylate form); the plasma concentration of *N*-desmethyl topotecan, an active metabolite of topotecan[20]; the total urinary concentration of topotecan; and the total urinary concentration of *N*-desmethyl topotecan were determined by high-performance liquid chromatography (HPLC) with fluorescence detection according to the method described by Rosing et al.[21] Briefly, separation was achieved on reversed-phase columns, and detection was performed fluorometrically with excitation of 380 nm and emission of 527 nm. The lower limit for quantitative determination of topotecan in plasma (lactone and total topotecan) and in urine was 0.22 nmol/L and 55 nmol/L, respectively, and the limit for *N*-desmethyl topotecan in plasma (lactone and total topotecan) and urine was 0.23 nmol/L and 5.6 nmol/L, respectively.

Pharmacokinetic and Pharmacodynamic Analyses

The following noncompartmental and two-compartmental pharmacokinetic parameters of topotecan and *N*-desmethyl topotecan were estimated by using WinNonlin®, Version 4.1 software (Pharsight Corporation; Mountain View, CA). C_{max} is the maximum drug concentration; $AUC0\text{-}_{\infty}$ is the area under the concentration-time curve calculated by the linear trapezoidal rule from time 0 to the last measurable data point and extrapolation to infinity. The elimination rate constant (λz) was determined by log-linear regression analysis of the terminal phase of the plasma concentration-time curves. The terminal half-lives ($T_{1/2}$) were calculated by using the formula: $T_{1/2} = 0.693/\lambda z$. Mean residence time (MRT) was calculated by the equation of AUMC (area under the first moment–time curve)/AUC-[infusion time]/2. Clearance (Cl) was calculated by dividing the dose received by the AUC. The volume of distribution at steady state (V_{ss}) was calculated by using the formula: $V_{ss} = CL \times MRT$. The urinary excretion (Ae; percent of dose) was calculated as amount excreted in urine/dose, and renal clearance

Table 3 Most Severe Toxicities at Different Dose Levels

Toxicity	Previously Treated Group								Previously Untreated Group							
	4 mg/m² (n = 3)				6 mg/m² (n = 3)				6 mg/m² (n = 3)				8 mg/m² (n = 3)			
	Grade				Grade				Grade				Grade			
	1	2	3	4	1	2	3	4	1	2	3	4	1	2	3	4
Hematologic Toxicity																
Leukopenia	0	2	1	0	0	2	0	1	1	1	1	0	0	2	1	0
Neutropenia	0	1	2	0	0	0	2	1	0	1	2	0	0	0	2	1
Thrombocytopenia	2	0	0	0	1	1	1	0	1	1	0	0	2	1	0	0
Anemia	0	1	2	0	0	3	0	0	0	2	1	0	0	2	1	0
Nonhematologic Toxicity																
Abnormal liver function (ALT or AST)	2	0	0	0	0	0	0	0	0	0	0	0	0	0	0	0
Abnormal renal function	0	0	0	0	0	0	0	0	0	0	0	0	0	0	0	0
Hypokalemia	0	0	0	0	1	0	0	0	1	0	0	0	0	0	0	1
Anorexia	1	0	1	1	0	3	0	0	2	0	1	0	3	0	0	0
Nausea	0	2	0	0	0	3	0	0	0	1	0	0	0	1	0	0
Vomiting	0	1	0	0	0	2	0	0	0	1	0	0	1	0	0	0
Fatigue	0	0	1	1	1	2	0	0	2	0	0	0	3	0	0	0
Weight loss	1	0	0	0	0	0	0	0	0	0	0	0	1	0	0	0
Diarrhea	1	0	0	0	0	0	0	0	1	0	0	0	0	0	0	0
Constipation	0	1	0	0	0	0	0	0	0	0	0	0	0	0	0	0
Urticaria	0	0	0	0	0	0	0	0	0	0	0	0	0	1	0	0
Stomatitis	0	0	0	0	1	0	0	0	1	0	0	0	1	0	0	0
Alopecia	0	0	0	0	0	1	0	0	1	0	0	0	3	0	0	0
Dyspnea	0	0	0	0	0	1	0	0	0	0	0	0	0	0	0	0
Febrile neutropenia	0	0	0	0	0	0	1	0	0	0	0	0	0	0	0	0
Fever	0	1	0	0	1	1	0	0	1	0	0	0	1	0	0	0
Fever (allergic reaction)	0	0	0	0	0	0	0	0	0	0	0	0	0	1	0	0
Infection with neutropenia	0	0	0	0	0	0	2	0	0	0	1	0	0	0	0	0

Abbreviations: ALT = alanine aminotransferase; AST = aspartate aminotransferase

(CLr) was calculated as total Ae/AUC. Additional pharmacokinetic parameters were estimated where appropriate using a two-compartment IV model such as time to reach maximum plasma concentration (T_{max}). The percent change in neutrophil count was calculated using the formula: percent change in neutrophil count = ([pretreatment count - nadir count]/pretreatment count) × 100.[22] The pharmacokinetic–pharmacodynamic correlations between the percent changes in neutrophil count and C_{max} or AUC_{∞} values for topotecan lactone were evaluated by using a simple maximum-effect (E_{max}) model and WinNonlin software, Version 5.2.1.

Results

During the period between March 1999 and November 2000, 12 patients participated in this study. The profile of the patient population is shown in Table 1. Three patients were women, and 9 were men, and their median age was 63 years (range, 53-68 years). All patients had a performance status of 1. A total of 20 courses of therapy were given in this study. The number of treatment cycles administered per patient was 1 or 2 (1 cycle in 4 patients, and 2 cycles in 8 patients). All patients were assessed for toxicity and response.

Toxicities

Maximum Tolerated Dose. One of the major toxicities observed during this study was myelosuppression, principally manifested by neutropenia. First, 3 previously treated patients were enrolled at dose level 1 (topotecan 4 mg/m² on days 1, 8 and 15). No DLT was observed during the first course at dose level 1. Febrile neutropenia and infection with grade 3/4 neutropenia were the DLT at the second dose level (topotecan 6 mg/m²) in the first cycle in all 3 patients who had received previous chemotherapy (Table 2). Because severe myelotoxicity was observed in the previously treated patients at this dose, only previously untreated patients were subsequently enrolled at the second dose level (topotecan 6 mg/m²). At this dose level the 3 previously untreated patients did not experience any DLT. However, at the 8-mg/m² level, grade 4 neutropenia > 3 days was observed in 1 patient, forcing a skipping of the topotecan dose on

Table 4 Pharmacokinetic Parameters of the Lactone Form of Topotecan and Total Topotecan Determined on Day 1

Parameter	Previously Treated Group						Previously Untreated Group					
	4 mg/m² (n = 3)			6 mg/m² (n = 3)			6 mg/m² (n = 3)			8 mg/m² (n = 3)		
Lactone	**Mean**		**SD**	**Mean**		**SD**	**Mean**		**SD**	**Mean**		**SD**
C_{max}, nmol/L	171.43	±	49.66	351.88	±	112.64	271.45	±	217.73	484.16	±	87.88
T_{max}, h	0.55	±	0.06	0.51	±	0.02	0.50	±	0.07	0.51	±	0.01
$AUC0_{-\infty}$, nmol·h/L	264.59	±	65.21	427.22	±	71.39	345.16	±	190.69	546.55	±	118.69
(%)[a]	(35)	±	(2)	(33)	±	(4)	(36)	±	(6)	(38)	±	(1)
$T_{1/2}$, h	5.37	±	0.65	4.92	±	0.69	5.62	±	0.34	4.84	±	0.13
λz, 1/h	0.1303	±	0.0162	0.1427	±	0.0187	0.1237	±	0.0077	0.1432	±	0.0038
MRT, h	3.53	±	0.40	3.14	±	1.01	3.47	±	0.69	2.46	±	0.14
Cl, L/h	55.28	±	17.62	49.36	±	9.89	71.32	±	45.94	49.72	±	11.41
V_{ss}, L	195.78	±	69.11	160.76	±	83.02	267.62	±	216.67	121.03	±	21.63
Total												
C_{max}, nmol/L	241.10	±	61.06	557.82	±	48.57	344.98	±	210.54	682.16	±	111.44
T_{max}, h	0.55	±	0.06	0.51	±	0.02	0.50	±	0.07	0.51	±	0.01
$AUC0_{-\infty}$, nmol·h/L	749.95	±	157.56	1305.37	±	172.72	913.08	±	385.60	1426.81	±	270.27
$T_{1/2}$, h	4.90	±	0.84	4.85	±	0.75	5.08	±	0.19	4.69	±	0.40
λz, 1/h	0.1442	±	0.0234	0.1451	±	0.0226	0.1366	±	0.0052	0.1485	±	0.0127
MRT, h	4.52	±	0.60	4.35	±	0.87	4.60	±	0.06	3.69	±	0.19
Cl, L/h	19.22	±	5.26	15.99	±	2.16	24.14	±	11.74	18.91	±	3.92
V_{ss}, L	85.54	±	18.61	69.11	±	14.56	111.44	±	55.59	69.26	±	11.14

[a]Lactone form as a percentage of total topotecan.
Abbreviations: λz = elimination rate constant; $AUC0_{-\infty}$ = area under the plasma concentration-time curve extrapolated to infinity; Cl = total body clearance; C_{max} = maximum concentration; MRT = mean residence time; $T_{1/2}$ = half-life in terminal phase; T_{max} = time to reach C_{max}; V_{ss} = volume of distribution at steady state

day 15. Another patient exhibited grade 3 neutropenia on day 15, and that also made it necessary to skip the topotecan dose scheduled for that day. Although only 1 DLT was observed at that dose level in the previously untreated patients, the dose of topotecan on day 15 was skipped in 2 of the 3 untreated patients because of hematologic toxicity; therefore, the MTD was estimated to be 8 mg/m², and the recommended dose was estimated to be 6 mg/m². No further attempts were made to increase the dose.

Hematologic Toxicity. Table 3 shows the most severe toxicities experienced during treatment. Although there was no grade 4 neutropenia at dose level 1 (4 mg/m²), short-lived grade 4 leukopenia and neutropenia occurred in 1 of the 3 previously treated patients at dose level 2 (6 mg/m²). No grade 4 leukopenia or neutropenia was observed in the 3 chemotherapy-naive patients at dose level 2. At the 8-mg/m² dose level, 1 of the 3 patients experienced grade 4 neutropenia > 3 days. Ten episodes of grade 3/4 neutropenia were reported during this trial, and 8 (80%) episodes were asymptomatic, whereas 2 episodes (20%) were associated with fever. The median time to the neutrophil nadir in the 12 patients who developed neutropenia during the first course was 21 days, and the median times to recovery ranged from 5 to 8 days.

Nadir platelet counts were observed from day 14 to day 17, and the median times to recovery ranged from 2 to 6.5 days. Topotecan generally had a mild effect on platelets, and only 1 course in the study (6 mg/m²) was associated with grade 3 thrombocytopenia (Table 3). Anemia was relatively common, and grade 3 anemia occurred in 4 (33%) of the patients.

Nonhematologic Toxicity. Overall, nonhematologic toxicities were infrequent and mild to moderate in severity (Table 3). Anorexia was the most frequent nonhematologic toxic effect. All patients experienced some degree of appetite loss. Grade ≥ 3 anorexia was reported in 3 (25%) of the patients. Toxicities ≥ grade 3 consisted of hypokalemia (n = 1), fatigue (n = 2), fabrile neutropenia (n = 1), and infection (n = 2). Other toxicities were < grade 3. There were no treatment-related deaths during this study.

Pharmacokinetics

Plasma samples for topotecan were obtained from all 12 patients during their first course of treatment. The plasma concentration-time curves for the different doses of topotecan are shown in Figure 1, and the pharmacokinetic parameters derived from the plotted data are listed in Table 4 and Table 5. The plasma concentrations of topotecan lactone and total topotecan reached their C_{max} at the end of the infusion, and the C_{max} values increased in proportion to the dose. The plasma concentration-time curves for topotecan lactone and total topotecan were fit by a biexponential model with a terminal half-life of 4.84-5.62 hours and 4.69-5.08 hours, respectively. *N*-desmethyl topotecan was rapidly formed from the parent

Figure 1 Plasma Concentration-Time Curves of Topotecan and Its Active Metabolite, N-Desmethyl Topotecan, in Patients Receiving Weekly Topotecan

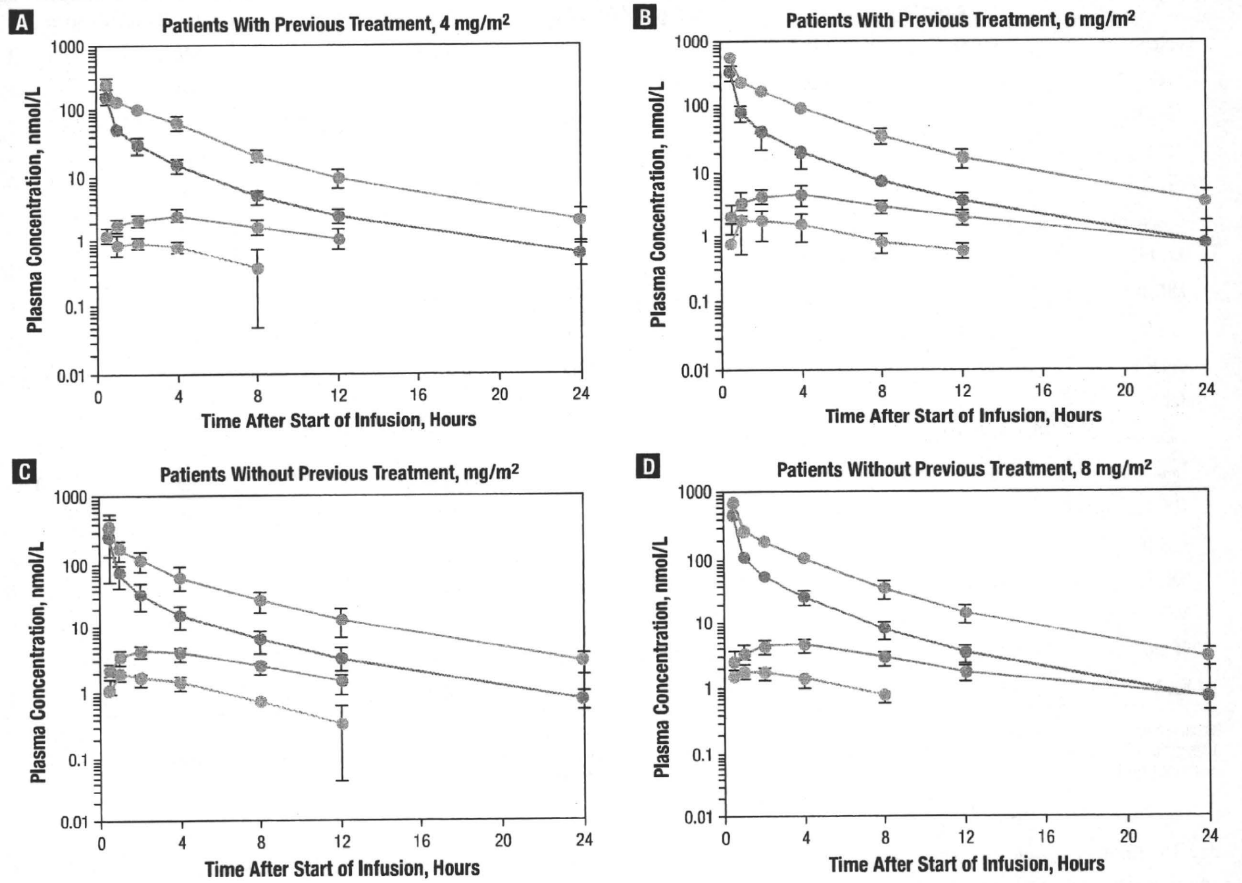

Each point represents the mean ± SD of the values in 4 patients. The open circles and closed circles represent the lactone form of topotecan and total topotecan, respectively, and the open triangles and closed triangles represent the lactone form of *N*-desmethyl topotecan and total *N*-desmethyl topotecan, respectively.

compound, and the C_{max} of *N*-desmethyl topotecan was reached between 1 hour and 4 hours after the start of the topotecan infusion. The plasma concentration of the metabolite decreased more slowly than that of topotecan, and its half-life ranged between 5 hours and 9 hours. No significant differences in pharmacokinetic parameters were observed between the previously treated group and the previously untreated group at the 6-mg/m² dose. The ratio of the C_{max} of the metabolite to that of topotecan ranged from 0.4% to 1.3%. Half-lives, V_{ss}, Cl, and urinary excretion also remained relatively constant over the range of doses administered. The mean V_{ss} for topotecan lactone was 121.03-267.62 L, and the mean Cl was 49.36-71.32 L/h. The ratio of the AUC_{∞} of topotecan lactone to that of total topotecan was approximately 35%. The mean urinary excretion ratio of topotecan and *N*-desmethyl topotecan over 48 hours at each dose ranged from 43.9% to 47.6% and from 1.8% to 2.7%, respectively.

Pharmacodynamics

The relationships between the percentage decrease in neutrophil count and both the C_{max} and AUC_{∞} values for topotecan lactone were well described by a simple E_{max} model (Figure 2). With this model, E_{max} and EC_{50} C_{max} were estimated for C_{max} as 90.6 ± 7.4% and 30.2 ± 20.8 nmol/L, respectively, and were estimated for $AUC_{0-\infty}$ as 99.7 ± 12.3% and 83.7 ± 53.5 nmol·hr/L, respectively.

Response

All 12 patients were assessed for response. No partial responses (PRs) or complete responses (CRs) were achieved in either the previously untreated group or the previously treated group. Two of the 10 patients with no change showed a minor response. One of them was a 67-year-old man treated at 6 mg/m² who had previously undergone combination therapy consisting of cisplatin plus vindesine and with whom a 25% reduction of the predefined target lesions was observed on day 23 and lasted 30 days. The other patient was a 68-year-old chemotherapy-naive man treated with the 6-mg/m² dose with whom a maximum reduction of 60% of his primary tumors were observed on day 18 and lasted 4 weeks, a 19.5% decrease in mediastinal lymph nodes were observed on day 46, and complete resolution of a pulmonary metastasis (14.1 mm × 12.8 mm) previously seen on CT scans were observed on day 18

Table 5 Pharmacokinetic Parameters of *N*-Desmethyl Topotecan (Total and Lactone Form) Determined on Day 1

Parameter	Previously Treated Group						Previously Untreated Group					
	4 mg/m² (n = 3)			6 mg/m² (n = 3)			6 mg/m² (n = 3)			8 mg/m² (n = 3)		
Lactone	**Mean**		**SD**	**Mean**		**SD**	**Mean**		**SD**	**Mean**		**SD**
C_{max}, nmol/L	1.01	±	0.20	1.98	±	1.19	2.03	±	0.45	1.83	±	0.34
T_{max}, h	2.34	±	1.59	1.67	±	0.58	1.00	±	0.00	1.18	±	0.76
$AUC0_{-\infty}$, nmol·h/L	11.76	±	0.43	18.88	±	6.47	15.36	±	1.98	17.10	±	0.83
(%)[a]	(37)	±	(10)	(28)	±	(4)	(33)	±	(4)	(27)	±	(1)
$T_{1/2}$, h	7.16	±	1.09	6.50	±	2.31	4.94	±	1.64	5.59	±	0.94
λz, 1/h	0.0982	±	0.0138	0.1148	±	0.0346	0.1495	±	0.0419	0.1264	±	0.0207
MRT, h	11.21	±	1.58	9.95	±	3.35	7.48	±	2.29	8.35	±	1.47
Total												
C_{max}, nmol/L	2.75	±	0.54	4.89	±	1.53	4.37	±	0.54	4.57	±	0.68
T_{max}, h	3.34	±	1.23	3.33	±	1.15	2.00	±	0.00	4.01	±	0.01
$AUC0_{-\infty}$, nmol·h/L	33.79	±	10.84	66.98	±	13.34	47.33	±	11.29	63.67	±	5.56
$T_{1/2}$, h	6.43	±	1.35	7.97	±	1.37	5.59	±	1.99	8.86	±	1.21
λz, 1/h	0.1108	±	0.0216	0.0885	±	0.0142	0.1338	±	0.0415	0.0792	±	0.0115
MRT, h	10.27	±	2.04	11.97	±	1.95	8.79	±	2.54	12.51	±	1.82

[a]Lactone form as a percentage of total topotecan.
Abbreviations: λz = elimination rate constant; $AUC0_{-\infty}$ = area under the plasma concentration-time curve extrapolated to infinity; C_{max} = maximum concentration; MRT = mean residence time; $T_{1/2}$ = half-life in terminal phase; T_{max} = time to reach C_{max}

and lasted 1 month. However, a left axillary node became palpable on day 46. The remaining 2 patients had disease progression.

Discussion

The standard regimen of topotecan of 1.5 mg/m²/day on days 1-5 of a 21-day cycle is an efficacious regimen for the treatment of patients with several malignant diseases, including relapsed epithelial ovarian cancer and SCLC.[6,23-25] Although topotecan on this schedule is generally well tolerated, patients heavily pretreated with platinum-based regimens may sometimes be susceptible to severe hematologic toxicities.[6,12] Furthermore, 5 daily infusions in an office or treatment center may be inconvenient for the patients. Weekly administration is one of the candidates for alternate dosing regimens to reduce toxicity without compromising efficacy. Preclinical studies in NSCLC cell lines demonstrate that with prolonged exposure to topotecan, topoisomerase I levels decreased but also appeared to return to baseline levels after 1 week, suggesting that a weekly regimen may target cells when they are most vulnerable to this agent.[7] In light of this information, we conducted this phase I and pharmacokinetic study of topotecan for the treatment of patients with advanced NSCLC.

This trial demonstrated that 8 mg/m² per week every 3 weeks was estimated to be the MTD because administration of topotecan on day 15 in 2 of 3 untreated patients was skipped because of hematologic toxicity, although 1 of 3 previously untreated patients experienced DLT at this dose level (Table 2). Therefore, for patients without previous chemotherapy, 6 mg/m² per week every 4 weeks was the recommended dose for further phase II trials. The dose-intensity possible with this schedule in previously untreated patients was 4.5 mg/m²/week. In patients with previous chemotherapy, the appropriate dose for this regimen was 4 mg/m² per week every 3 weeks, with dose intensity of 3 mg/m²/week. This favorably compares the dose intensity of 2.5 mg/m²/week achievable with the standard regimen of 1.5 mg/m² daily for 5 days every 3 weeks. The recommended dose of 4 mg/m²/week for previously treated patients was consistent with other studies in ovarian cancer with this schedule.[8,10,26,27] Homesley et al first reported a phase I/II study of weekly intravenous bolus topotecan in patients with recurrent ovarian cancer, starting at 1.5 mg/m² and escalating at 0.5 mg/m² increments every 3 weeks.[8] The MTD and recommended dose was determined to be 4 mg/m² per week every 3 weeks in previously treated patients, with the DLTs being anemia, chronic fatigue, and gastrointestinal toxicities including nausea, and vomiting. Myelosuppression was rarely dose limiting. In contrast, in our trial, myelosuppression was frequently dose limiting (Table 2). As expected, the degree of myelosuppression was related to the patient's pretreatment status. At dose level of 6 mg/m²/week in previously treated patients, 1 case of grade 3 neutropenic fever and 2 cases of infection with grade 3 neutropenia were observed as the DLTs. At dose level of 8 mg/m²/week in patients with no previous chemotherapy, treatment omission on day 15 because of neutropenia was dose limiting in 2 patients. Nonhematologic toxic effects ≥ grade 3 consisted of anorexia (3 patients), fatigue (2 patients), and infection with neutropenia (3 patients; Table 3). These toxicities were predictable, reversible and manageable. The spectrum of toxicities for weekly topotecan was similar to that of the standard daily for 5 days regimen.[28,29]

Topotecan pharmacokinetics were similar to those reported in previous studies.[28,30] After cessation of infusion, the topotecan curves showed a biexponential decay (Figure 1). In accordance with

Figure 2 Pharmacodynamic Modeling of the Percent Change in Neutrophil Count Versus C_{max} or AUC_{∞} of Topotecan Lactone by Means of a Simple Maximum-Effect Model

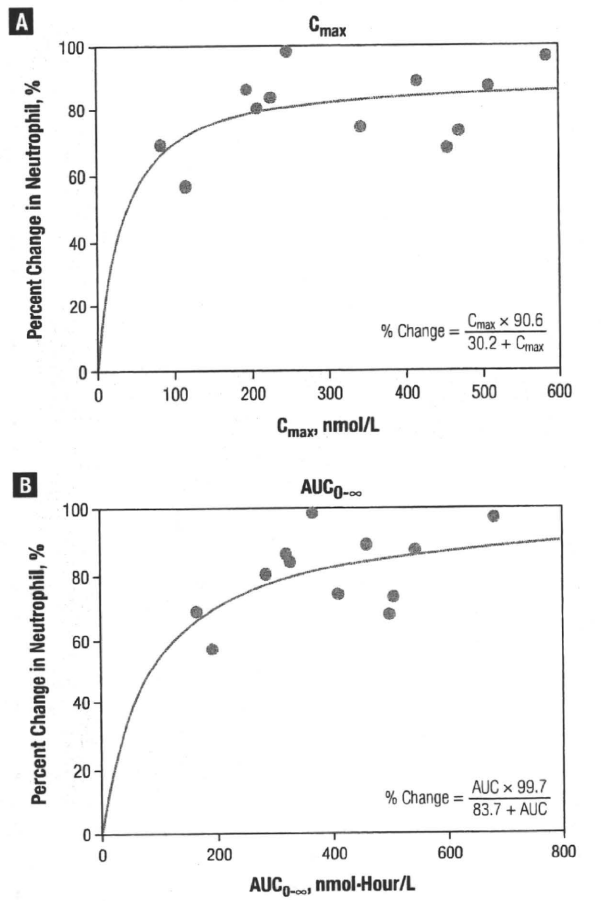

the report by van Warmerdam et al,[30] after about 1.5 hours the concentration of the lactone form and the carboxylate form declined in parallel, with identical slopes. Mean topotecan C_{max} and AUC_{∞} increased linearly with doses in the dose range used for both lactone and total drug (Table 4). Curtis et al reported the pharmacokinetic study of topotecan,[31] in which patients with previously treated cancer were administered topotecan at the same dose (4 mg/m^2) as in our trial. Their study included 16 white patients. A comparison of the pharmacokinetic parameters of total topotecan in their study and our trial (Table 5) showed similar results: C_{max} (144 ng/mL vs. 110.4 ng/mL; 314 nmol/L vs. 241.1 nmol/L), $AUC_{0-\infty}$ (372 ng·h/mL vs. 343.4 ng·h/mL; 812 nmol·h/L vs. 750 nmol·h/L), $T_{1/2}$ (5 h vs. 4.9 h), Cl (20.6 L/h vs. 19.2 L/h), and V_{ss} (101 L vs. 85.5 L), respectively. The toxicity profile of topotecan in our trial was also similar to that in their study. Thus, there seems to be no need to consider pharmacogenomic differences between white and Japanese patients. Herben et al first reported the pharmacokinetics of *N*-desmethyl topotecan.[32] Its formation is consistent with a hydroxylation step catalyzed by the cytochrome P450 system. This metabolite is supposed to have equal or slightly less antitumor activity compared with topotecan.[20,33] *N*-desmethyl topotecan appeared in plasma after the end of topotecan infusion, with lag time of 0.58 ± 0.24 hours. The time to reach maximal plasma concentration was 3.4 ± 1.0 hours. The metabolite-to-topotecan ratio of C_{max} was about 0.5%. The 24-hour urinary recovery of the metabolite was 1.4 ± 0.6% of the topotecan dose administered. In our trial, the metabolite was already detected at the end of infusion (Figure 1). Although plasma concentrations of topotecan began to decline at the end of the infusion, those of the metabolite increased initially, and the maximal plasma levels were reached from 0.5 to 4 hours after the end of the infusion, with the half-lives from 4 to 10 hours. Recovery within 48 hours of the metabolite in the urine was 1.8%-2.7% of the topotecan dose administered. The severity of neutropenia was more closely related to the AUC of topotecan than to C_{max} of topotecan. The percentage decrease in ANC is primarily dependent on systemic exposure to topotecan. The pharmacodynamic curves suggest that the percent change in neutrophils may peak when topotecan is administered at a dose lower than 4 mg/m^2 (Figure 2). However, a review of previously published papers suggests that the weekly dose of 4 mg/m^2 is appropriate.[8-11,15,31]

Neither CR nor PR was obtained during this phase I trial, although 2 patients showed a minor response. It is of note that the proportion of patients with stable disease was very high (80%), and this point is important because the disease stabilization may be of benefit for the survival of patients. However, the number of patients in this study is too small to draw any valid conclusion about the ultimate clinical activity of this weekly regimen.

Conclusion

This study showed that 6 mg/m^2 and 4 mg/m^2 were the recommended doses of weekly topotecan for further study in previously untreated and previously treated patients, respectively. The major DLT were febrile neutropenia, infection, and grade 4 neutropenia ≥ 3 days. Because of its more improved patient convenience and its generally mild toxicity profile, the weekly regimen may provide an attractive alternative to the US Food and Drug Administration (FDA)–approved 5-day schedule regimen in patients with lung cancer.

It is not clear whether chemotherapy-naive patients will benefit from this treatment given the lack of response to single-agent topotecan. Treatment of platinum-doublet chemotherapy should be recommended for these nonresponding patients with good performance status because platinum-based doublet chemotherapy remains the cornerstone of therapy in the first-line setting in advanced NSCLC.[34]

Based on the results of this study, it was concluded that 6 mg/m^2 and 4 mg/m^2 should be the recommended doses of weekly topotecan for further study in previously untreated patients and previously treated patients, respectively. The major DLTs were febrile neutropenia, infection, and grade 4 neutropenia ≥ 3 days. Because of its greater convenience for patients and its generally mild toxicity profile, the weekly regimen may provide an attractive alternative to the FDA-approved 5-day schedule regimen for patients with lung cancer.

Acknowledgments

The authors would like to thank Mr. Takashi Kawashiro for his

help with the preparation of the manuscript and the pharmacokinetic analysis.

Disclosures

Akihira Mukaiyama and Pascal Yoshida are employees of and hold stock or equity ownership in GlaxoSmithKline. Hiroaki Arase is an employee of GlaxoSmithKline. All other authors have no relevant relationships to disclose.

References

1. Wall ME, Wani MC, Cook CE, et al. Plant antitumor agents. I. The isolation and structure of camptothecin, a novel alkaloidal leukemia and tumor inhibitor from camptotheca acuminata. *J Am Chem Soc* 1966; 88:3888-90.
2. Hsiang YH, Hertzberg R, Hecht S, et al. Camptothecin induces protein-linked DNA breaks via mammalian DNA topoisomerase I. *J Biol Chem* 1985; 260:14873-8.
3. Andoh T, Ishii K, Suzuki Y, et al. Characterization of a mammalian mutant with a camptothecin-resistant DNA topoisomerase I. *Proc Natl Acad Sci USA* 1987; 84:5565-9.
4. Hertzberg RP, Caranfa MJ, Hecht SM. On the mechanism of topoisomerase I inhibition by camptothecin: evidence for binding to an enzyme-DNA complex. *Biochemistry* 1989; 28:4629-38.
5. Hsiang YH, Lihou MG, Liu LF. Arrest of replication forks by drug-stabilized topoisomerase I-DNA cleavable complexes as a mechanism of cell killing by camptothecin. *Cancer Res* 1989; 49:5077-82.
6. von Pawel J, Schiller JH, Shepherd FA, et al. Topotecan versus cyclophosphamide, doxorubicin, and vincristine for the treatment of recurrent small-cell lung cancer. *J Clin Oncol* 1999; 17:658-67.
7. Bence A, Mattingly C, Desimone P, et al. Evaluation of topotecan cytotoxicity and topoisomerase I levels in non-small cell lung cancer cells. *Proc Am Assoc Cancer Res* 2002; 43:247 (abstract 1227).
8. Homesley HD, Hall DJ, Martin DA, et al. A dose-escalating study of weekly bolus topotecan in previously treated ovarian cancer patients. *Gynecol Oncol* 2001; 83:394-9
9. Bhoola SM, Coleman RL, Herzog T, et al. Retrospective analysis of weekly topotecan as salvage therapy in relapsed ovarian cancer. *Gynecol Oncol* 2004; 95:564-9.
10. Levy T, Inbar M, Menczer J, et al. Phase II study of weekly topotecan in patients with recurrent or persistent epithelial ovarian cancer. *Gynecol Oncol* 2004; 95:686-90.
11. O'Malley DM, Azodi M, Makkenchery A, et al. Weekly topotecan in heavily pretreated patients with recurrent epithelial ovarian carcinoma. *Gynecol Oncol* 2005; 98:242-8.
12. Rowinsky EK. Weekly topotecan: an alternative to topotecan's standard daily x 5 schedule? *Oncologist* 2002; 7:324-30.
13. Safra T, Menczer J, Bernstein R, et al. Efficacy and toxicity of weekly topotecan in recurrent epithelial ovarian and primary peritoneal cancer. *Gynecol Oncol* 2007; 105:205-10.
14. Largillier R, Valenza B, Ferrero JM, et al. Haematological evaluation of weekly therapy with topotecan for the treatment of recurrent ovarian cancer resistant to platinum-based therapy. *Oncology* 2007; 73:177-84.
15. Morris R, Alvarez RD, Andrews S, et al. Topotecan weekly bolus chemotherapy for relapsed platinum-sensitive ovarian and peritoneal cancers. *Gynecol Oncol* 2008; 109:346-52.
16. Puls LE, Phillips B, Schammel C, et al. A phase I-II trial of weekly topotecan in the treatment of recurrent cervical carcinoma. *Med Oncol* 2009; 27:368-72.
17. Fiorica JV, Blessing JA, Puneky LV, et al. A Phase II evaluation of weekly topotecan as a single agent second line therapy in persistent or recurrent carcinoma of the cervix: a Gynecologic Oncology Group study. *Gynecol Oncol* 2009; 115:285-9.
18. Mountain CF. Revisions in the International System for Staging Lung Cancer. *Chest* 1997; 111:1710-7.
19. Miller AB, Hoogstraten B, Staquet M, et al. Reporting results of cancer treatment. *Cancer* 1981; 47:207-14.
20. Rosing H, Herben VM, van Gortel-van Zomeren DM, et al. Isolation and structural confirmation of N-desmethyl topotecan, a metabolite of topotecan. *Cancer Chemother Pharmacol* 1997; 39:498-504.
21. Rosing H, van Zomeren DM, Doyle E, et al. Quantification of topotecan and its metabolite N-desmethyl topotecan in human plasma, urine and faeces by high-performance liquid chromatographic methods. *J Chromatogr B Biomed Sci Appl* 1999; 727:191-203.
22. Holford NH, Sheiner LB. Kinetics of pharmacologic response. *Pharmacol Ther* 1982; 16:143-66.
23. Carmichael J, Ozols RF. Topotecan, an active new antineoplastic agent: review and current status. *Expert Opin Investig Drugs* 1997; 6:593-608.
24. ten Bokkel Huinink W, Carmichael J, Armstrong D, et al. Efficacy and safety of topotecan in the treatment of advanced ovarian carcinoma. *Semin Oncol* 1997; 24:S5-19-S15-25.
25. ten Bokkel Huinink W, Gore M, Carmichael J, et al. Topotecan versus paclitaxel for the treatment of recurrent epithelial ovarian cancer. *J Clin Oncol* 1997; 15:2183-93.
26. Morris R, Munkarah A. Alternate dosing schedules for topotecan in the treatment of recurrent ovarian cancer. *Oncologist* 2002; 7(suppl 5):29-35.
27. Abushahin F, Singh DK, Lurain JR, et al. Weekly topotecan for recurrent platinum resistant ovarian cancer. *Gynecol Oncol* 2008; 108:53-7.
28. Rowinsky EK, Grochow LB, Hendricks CB, et al. Phase I and pharmacologic study of topotecan: a novel topoisomerase I inhibitor. *J Clin Oncol* 1992; 10:647-56.
29. O'Brien M, Eckardt J, Ramlau R. Recent advances with topotecan in the treatment of lung cancer. *Oncologist* 2007; 12:1194-204.
30. van Warmerdam LJ, Verweij J, Schellens JH, et al. Pharmacokinetics and pharmacodynamics of topotecan administered daily for 5 days every 3 weeks. *Cancer Chemother Pharmacol* 1995; 35:237-45.
31. Curtis KK, Hartney JT, Jewell RC, et al. A phase I study to characterize the safety, tolerability, and pharmacokinetics of topotecan at 4 mg/m^2 administered weekly as a 30-minute intravenous infusion in patients with cancer. *J Clin Pharmacol* 2010; 50:268-75.
32. Herben VM, ten Bokkel Huinink WW, Dubbelman AC, et al. Phase I and pharmacological study of sequential intravenous topotecan and oral etoposide. *Br J Cancer* 1997; 76:1500-8.
33. Zamboni WC, Gajjar AJ, Heideman RL, et al. Phenytoin alters the disposition of topotecan and N-desmethyl topotecan in a patient with medulloblastoma. *Clin Cancer Res* 1998; 4:783-9.
34. Schiller JH, Harrington D, Belani CP, et al. Comparison of four chemotherapy regimens for advanced non-small-cell lung cancer. *N Engl J Med* 2002; 346:92-8.

Preclinical Development

Molecular Cancer Therapeutics

TAK-701, a Humanized Monoclonal Antibody to Hepatocyte Growth Factor, Reverses Gefitinib Resistance Induced by Tumor-Derived HGF in Non–Small Cell Lung Cancer with an *EGFR* Mutation

Wataru Okamoto[1], Isamu Okamoto[1], Kaoru Tanaka[1], Erina Hatashita[1], Yuki Yamada[1], Kiyoko Kuwata[1], Haruka Yamaguchi[1], Tokuzo Arao[2], Kazuto Nishio[2], Masahiro Fukuoka[3], Pasi A. Jänne[4,5], and Kazuhiko Nakagawa[1]

Abstract

Most non–small cell lung cancer (NSCLC) tumors with an activating mutation of the epidermal growth factor receptor (EGFR) are initially responsive to EGFR tyrosine kinase inhibitors (TKI) such as gefitinib but ultimately develop resistance to these drugs. Hepatocyte growth factor (HGF) induces EGFR-TKI resistance in NSCLC cells with such a mutation. We investigated strategies to overcome gefitinib resistance induced by HGF. Human NSCLC cells with an activating *EGFR* mutation (HCC827 cells) were engineered to stably express HGF (HCC827-HGF cells). HCC827-HGF cells secreted large amounts of HGF and exhibited resistance to gefitinib *in vitro* to an extent similar to that of HCC827 GR cells, in which the gene for the HGF receptor MET is amplified. A MET-TKI reversed gefitinib resistance in HCC827-HGF cells as well as in HCC827 GR cells, suggesting that MET activation induces gefitinib resistance in both cell lines. TAK-701, a humanized monoclonal antibody to HGF, in combination with gefitinib inhibited the phosphorylation of MET, EGFR, extracellular signal-regulated kinase, and AKT in HCC827-HGF cells, resulting in suppression of cell growth and indicating that autocrine HGF-MET signaling contributes to gefitinib resistance in these cells. Combination therapy with TAK-701 and gefitinib also markedly inhibited the growth of HCC827-HGF tumors *in vivo*. The addition of TAK-701 to gefitinib is a promising strategy to overcome EGFR-TKI resistance induced by HGF in NSCLC with an activating *EGFR* mutation. *Mol Cancer Ther; 9(10); 2785–92. ©2010 AACR.*

Introduction

Somatic mutations in the kinase domain of the epidermal growth factor receptor (EGFR) are associated with a high rate of response to EGFR tyrosine kinase inhibitors (TKI) such as gefitinib (Fig. 1) and erlotinib in advanced non–small cell lung cancer (NSCLC; refs. 1–3). Despite the therapeutic benefit of EGFR-TKIs in NSCLC, however, most patients ultimately develop resistance to these drugs. A secondary T790M mutation of *EGFR* and amplification of the *MET* gene are major causes of acquired resistance to EGFR-TKIs (4–7). In addition, hepatocyte growth factor (HGF), a ligand of the MET oncoprotein (8, 9), induces gefitinib resistance in *EGFR* mutation–positive NSCLC by activating MET and downstream signaling (10).

HGF was originally identified as a mitogenic protein for hepatocytes (11). Both HGF and its MET receptor are expressed, and often overexpressed, in a broad spectrum of human solid tumors including lung, mesothelioma, breast, and brain cancer (12–16). HGF thus acts as an autocrine or paracrine growth factor for these tumor cells (17, 18). TAK-701 is a potent humanized monoclonal antibody to HGF that blocks various HGF-induced biological activities as well as inhibits tumor growth in an autocrine HGF-MET–driven xenograft model.[6] To identify strategies or agents capable of overcoming resistance to EGFR-TKIs induced by HGF, we have now established sublines of the *EGFR* mutation–positive human NSCLC cell line HCC827 that stably express transfected HGF cDNA. With the use of these cells, we investigated the effects of TAK-701 on HGF-MET signaling and gefitinib resistance induced by cell-derived HGF both *in vitro* and *in vivo*.

Authors' Affiliations: Departments of [1]Medical Oncology and [2]Genome Biology, Kinki University School of Medicine, Osaka-Sayama, Osaka, Japan; [3]Cancer Center, Izumi City Hospital, Izumi, Osaka, Japan; and [4]Lowe Center for Thoracic Oncology and [5]Department of Medical Oncology, Dana-Farber Cancer Institute, Boston, Massachusetts

Corresponding Author: Isamu Okamoto, Department of Medical Oncology, Kinki University School of Medicine, 377-2 Ohno-higashi, Osaka-Sayama, Osaka 589-8511, Japan. Phone: 81-72-366-0221; Fax: 81-72-360-5000. E-mail: chi-okamoto@dotd.med.kindai.ac.jp

doi: 10.1158/1535-7163.MCT-10-0481

[6] Kitahara O, Nishizawa S, Ito Y, Toyoda Y, Misumi Y, Sato S, Inaoka T, Klakamp SL, Kokubo T, Hori A. TAK-701, a humanized monoclonal antibody to human hepatocyte growth factor, exhibits promising antitumor effects on multiple tumor types. In preparation.

Materials and Methods

Cell culture and reagents

The *EGFR* mutant NSCLC cell lines HCC827 (del E746_A750) and the human glioblastoma cell line U87MG were obtained from the American Type Culture Collection. HCC827 GR5 (del E746_A750/*MET* amplified) was generated and characterized as described previously (6). We screened all sublines of HCC827 for the presence of *EGFR* mutations by direct DNA sequencing of exons 18 to 21 and *MET* amplification by fluorescence *in situ* hybridization analysis with a probe specific for MET and a control probe for the centromere of chromosome 7 as described previously (19, 20) for this study. All cells were passaged for ≤3 months before the renewal from frozen, early-passage stocks obtained from the indicated sources. Cells were regularly screened for mycoplasma with the use of a MycoAlert Mycoplasma Detection Kit (Lonza). HCC827 cells were cultured under a humidified atmosphere of 5% CO_2 at 37°C in RPMI 1640 medium (Sigma) supplemented with 10% fetal bovine serum. HCC827 GR5 cells were cultured in RPMI 1640 medium supplemented with 10% fetal bovine serum and 1 μmol/L gefitinib. U87MG cells were cultured in DMEM (Gibco) supplemented with 10% fetal bovine serum. TAK-701 was kindly provided by Takeda Pharmaceutical Co. Ltd., gefitinib was obtained from AstraZeneca, and PHA-665752 was from Tocris Bioscience.

Cell transfection

A full-length cDNA fragment encoding human HGF was obtained from U87MG cells by reverse transcription and PCR with the primers HGF-F (5-GCGGCCGCAG-CACCATGTGGGTGACCAAA-3) and HGF-R (5-CGGGATCCCTATGACTGTGGTACCTTATAT-3). The amplification product was verified by sequencing after its cloning into the pCR-Blunt II-TOPO vector (Invitrogen). The HGF cDNA was excised from pCR-Blunt II-TOPO and transferred to the pQCXIH retroviral vector (Clontech). Retroviruses encoding HGF were then produced and used to infect HCC827 cells as described (21). Cells stably expressing HGF were then isolated by selection with hygromycin at 500 μg/mL (InvivoGen).

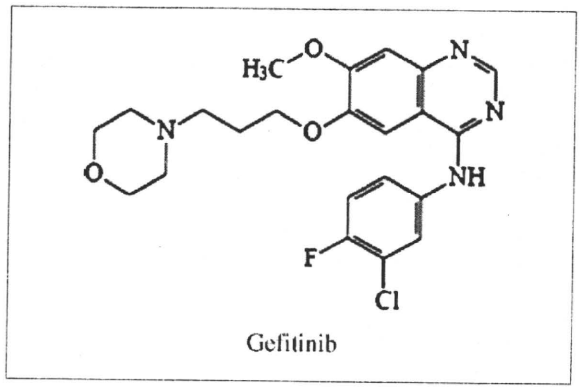

Gefitinib

Figure 1. The structure of gefitinib.

Enzyme-linked immunosorbent assay for HGF

Cells (5×10^5) were seeded in 6-well plates, cultured overnight in complete medium, and then incubated in serum-free medium for 24 hours, after which the latter medium was collected and assayed for HGF with a Human HGF Quantikine ELISA Kit (R&D Systems). A standard curve for the enzyme-linked immunosorbent assay (ELISA) was generated with the supplied reagents, and HGF concentration was determined as the average value from triplicate samples.

Cell growth inhibition assay

Cells were transferred to 96-well flat-bottomed plates and cultured for 24 hours before exposure for 72 hours to various concentrations of gefitinib, TAK-701, or PHA-665752, as indicated. Tetra Color One (5 mmol/L tetrazolium monosodium salt and 0.2 mmol/L 1-methoxy-5-methyl phenazinium methylsulfate; Seikagaku Kogyo) was then added to each well, and the cells were incubated for 3 hours at 37°C before measurement of absorbance at 490 nm with a Multiskan Spectrum instrument (Thermo Labsystems). Absorbance values were expressed as a percentage of that for untreated cells.

Annexin V binding assay

The binding of Annexin V to cells was measured with the use of an Annexin-V-FLUOS Staining Kit (Roche). Cells were harvested by exposure to trypsin-EDTA, washed with PBS, and centrifuged at 200 × *g* for 5 minutes. The cell pellets were resuspended in 100 μL of Annexin-V-FLUOS labeling solution, incubated for 10 to 15 minutes at 15°C to 25°C, and then analyzed for fluorescence with a flow cytometer (FACSCalibur) and Cell Quest software (Becton Dickinson).

Immunoblot analysis

Cells were washed twice with ice-cold PBS and then lysed with 1× cell lysis buffer (Cell Signaling Technology) consisting of 20 mmol/L Tris-HCl (pH 7.5), 150 mmol/L NaCl, 1 mmol/L EDTA (disodium salt), 1 mmol/L EGTA, 1% Triton X-100, 2.5 mmol/L sodium pyrophosphate, 1 mmol/L β-glycerophosphate, 1 mmol/L Na_3VO_4, leupeptin (1 μg/mL), and 1 mmol/L phenylmethylsulfonyl fluoride. The protein concentration of cell lysates was determined with a bicinchoninic acid protein assay kit (Thermo Fisher Scientific), and equal amounts of protein were subjected to SDS-PAGE on 7.5% gels (Bio-Rad). The separated proteins were transferred to a nitrocellulose membrane, which was then incubated with Blocking One solution (Nacalai Tesque) for 20 minutes at room temperature before incubation overnight at 4°C with primary antibodies. Antibodies to phosphorylated EGFR (phosphotyrosine-1068), to phosphorylated MET (phosphotyrosine-1349), to phosphorylated or total forms

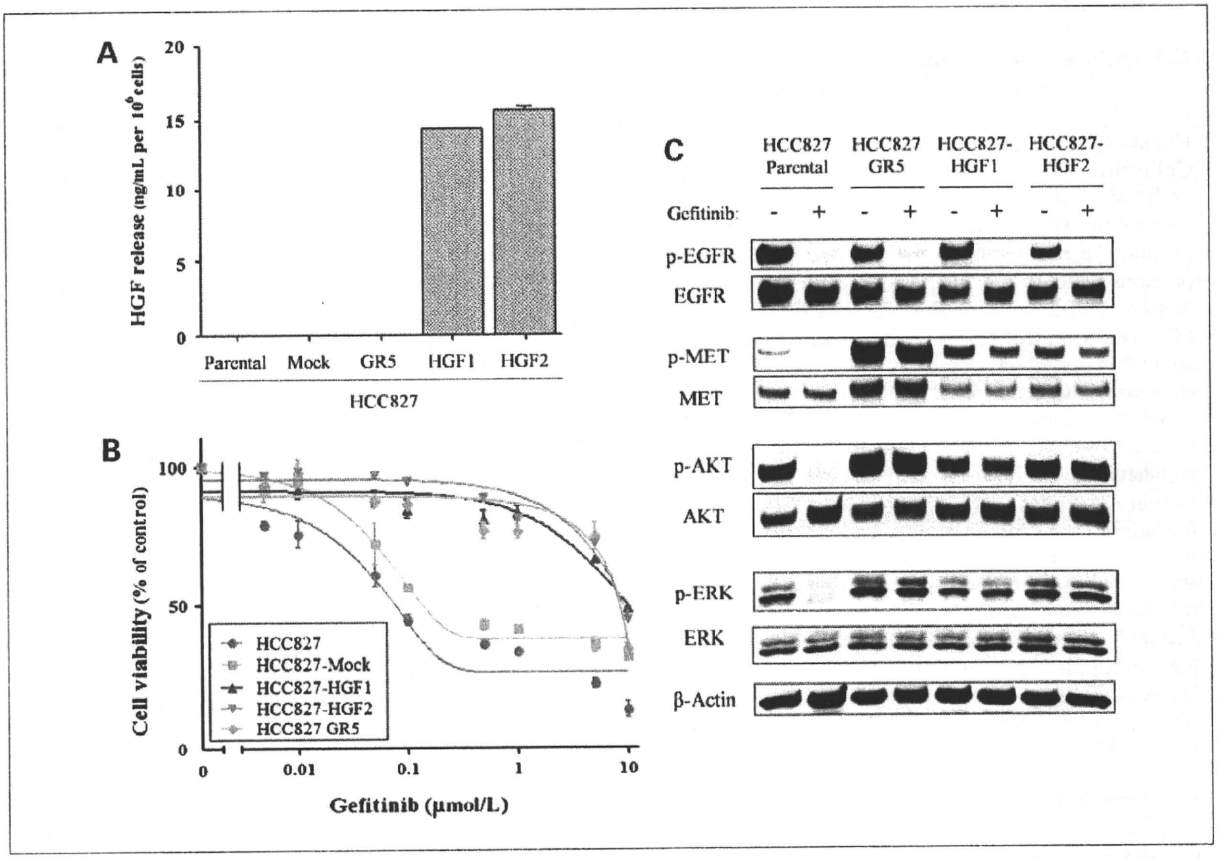

Figure 2. Characterization of HCC827 isogenic cell lines. A, HCC827 isogenic cell lines (HCC827, HCC827-Mock, HCC827-HGF1 and -HGF2, and HCC827 GR5) were cultured overnight in medium containing 10% serum and then incubated for 24 hours in serum-free medium, after which the culture supernatants were collected and assayed for HGF with an ELISA. Data are means ± SD from three independent experiments. B, HCC827 isogenic cell lines were cultured in medium containing 10% serum for 72 hours in the presence of various concentrations of gefitinib, after which cell viability was assessed as described in Materials and Methods. The number of viable cells is expressed as a percentage of the value for untreated cells. Data are means ± SD from three independent experiments. C, HCC827 isogenic cell lines were incubated for 1 hour with or without gefitinib (100 nmol/L) in medium containing 10% serum, after which the cells were lysed and subjected to immunoblot analysis with antibodies to phosphorylated (p-) or total forms of EGFR, MET, AKT, or ERK, or with those to β-actin (loading control).

of AKT, and to phosphorylated extracellular signal-regulated kinase (ERK) were obtained from Cell Signaling Technology; those to total ERK were from Santa Cruz Biotechnology; those to total EGFR and to total MET were from Zymed/Invitrogen; and those to β-actin were from Sigma. The membrane was then washed with PBS containing 0.05% Tween 20 before incubation for 1 hour at room temperature with horseradish peroxidase-conjugated secondary antibodies (GE Healthcare). Immune complexes were finally detected with ECL Western blotting detection reagents (GE Healthcare).

Growth inhibition assay *in vivo*

All animal studies were done in accordance with the Recommendations for Handling of Laboratory Animals for Biomedical Research compiled by the Committee on Safety and Ethical Handling Regulations for Laboratory Animal Experiments, Kinki University. The ethical procedures followed met the requirements of the United Kingdom Coordinating Committee on Cancer Research guidelines (22). HCC827 cells were implanted s.c. into the right hind leg of 6-week-old female athymic nude mice (BALB/c *nu/nu*; CLEA Japan). Tumor volume was determined from caliper measurement of tumor length (L) and width (W) according to the formula $LW^2/2$. Treatment was initiated when tumors in each group of animals achieved an average volume of 300 to 400 mm^3. Treatment groups (each containing five mice) consisted of vehicle control, TAK-701 alone, gefitinib alone, and TAK-701 plus gefitinib. The mice were injected with TAK-701 (5 mg/kg) i.p. twice a week for 7 weeks; control animals received PBS as vehicle. Gefitinib (50 mg/kg) was administered by oral gavage daily for 49 days; control animals received a 0.5% (w/v) aqueous solution of hydroxypropylmethylcellulose as vehicle. Both tumor size and body weight were measured twice per week.

Statistical analysis

The data, presented as means ± SD or SE, were analyzed with Student's two-tailed t test, with $P < 0.05$ considered statistically significant.

Results

Cell-derived HGF induces gefitinib resistance in *EGFR* mutation–positive NSCLC cells

To investigate whether cell-derived HGF induces gefitinib resistance in NSCLC cells with an *EGFR* mutation, we established HCC827 cells (which are *EGFR* mutation positive) that stably express human HGF (HCC827-HGF1 and -HGF2 cells) or stably harbor the corresponding empty vector (HCC827-Mock cells). The secretion of HGF from these cell lines as well as from the parental (HCC827) cells and from an HCC827 subline with *MET* amplification (HCC827 GR5) was examined with the use of an ELISA. We found that HCC827-HGF1 and -HGF2 cells released large amounts of HGF into the culture medium, whereas the secretion of HGF from parental (HCC827), HCC827-Mock, or HCC827 GR5 cells was undetectable (Fig. 2A). To assess the effects of gefitinib on cell growth, we exposed these five cell lines to various concentrations of the drug and then measured cell viability. HCC827 GR5 as well as HCC827-HGF1 and -HGF2 cells showed a reduced sensitivity to gefitinib compared with HCC827 and HCC827-Mock cells, with median inhibitory concentrations of ~10 μmol/L apparent for the former cell lines compared with ~0.1 μmol/L for the latter (Fig. 2B). To investigate possible differences in signal transduction among these cell lines, we examined the effects of gefitinib on EGFR, MET, AKT, and ERK phosphorylation by immunoblot analysis (Fig. 2C). In the parental cells, gefitinib markedly inhibited the phosphorylation of EGFR, AKT, and ERK. In contrast, in the resistant cells (HCC827 GR5, and HCC827-HGF1 and -HGF2), gefitinib alone had no effect on AKT and ERK phosphorylation, although it substantially reduced the level of EGFR phosphorylation. These data suggest that sustained AKT and ERK signaling in the presence of gefitinib contributes to gefitinib

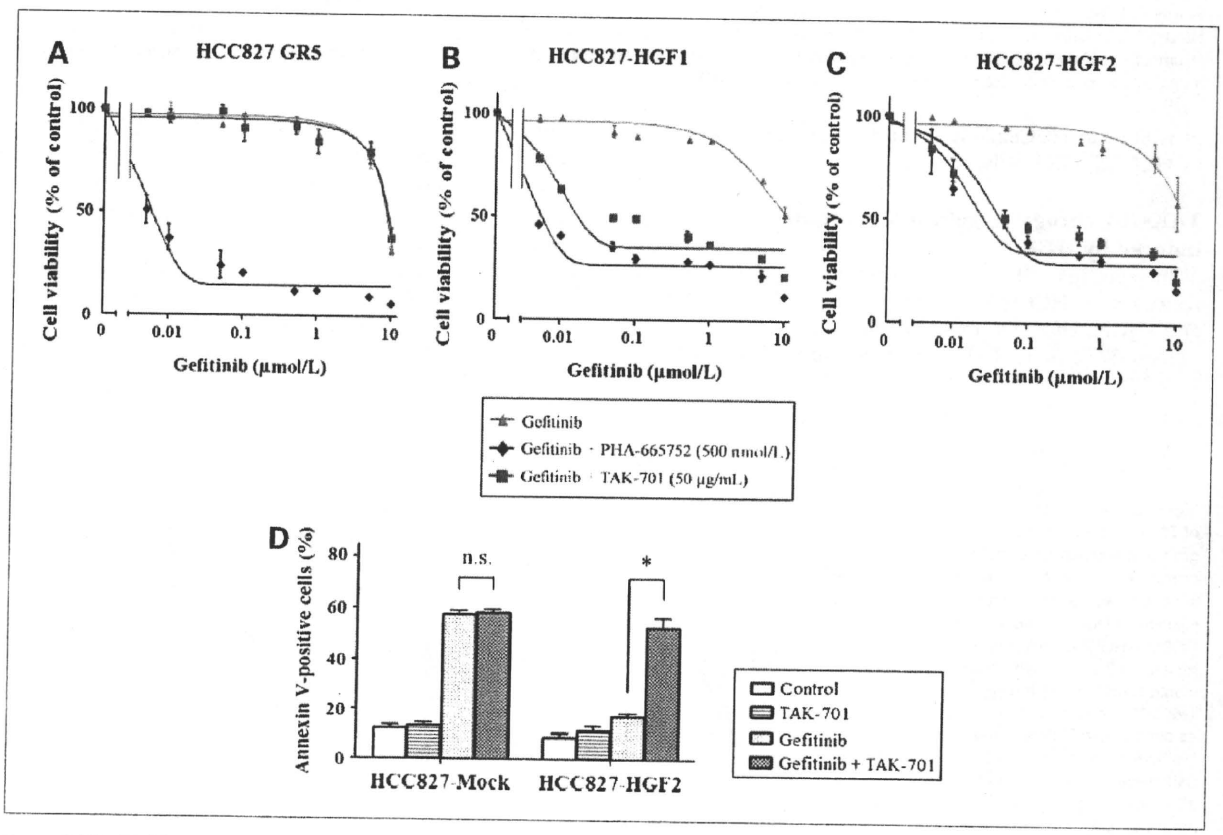

Figure 3. Effects of the combination of gefitinib and either TAK-701 or PHA-665752 on the growth of gefitinib-resistant NSCLC cells. A to C, HCC827 GR5 cells (A), HCC827-HGF1 cells (B), and HCC827-HGF2 cells (C) were cultured for 72 hours in medium containing 10% serum, various concentrations of gefitinib, and either PHA-665752 (500 nmol/L) or TAK-701 (50 μg/mL), after which cell viability was assessed. Data are means ± SD from three independent experiments. D, HCC827-Mock or HCC827-HGF2 cells were incubated in the absence or presence of gefitinib (1 μmol/L) or TAK-701 (50 μg/mL) for 48 hours in medium containing 10% serum. The proportion of apoptotic cells was then assessed by staining with Annexin V followed by flow cytometry. Data are means ± SD from three independent experiments. *$P < 0.001$; n.s., not significant.

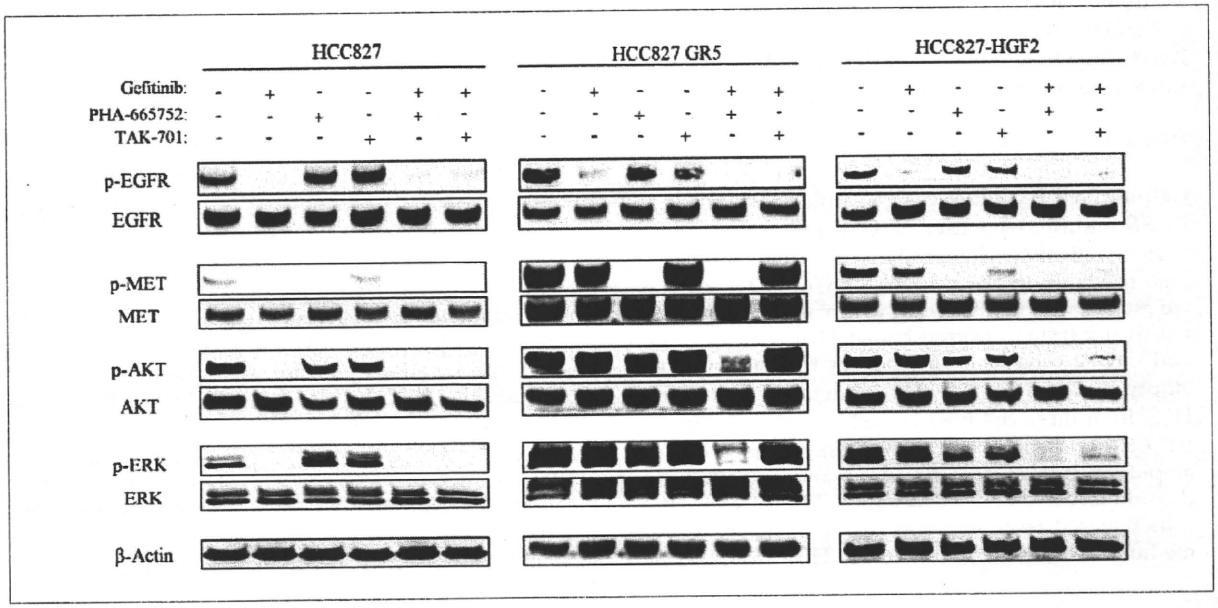

Figure 4. Effects of the combination of gefitinib and either TAK-701 or PHA-665752 on cell signaling in gefitinib-resistant NSCLC cells. HCC827 cells, HCC827 GR5 cells, and HCC827-HGF2 cells were incubated for 6 hours in medium containing 10% serum in the absence or presence of gefitinib (1 μmol/L), PHA-665752 (500 nmol/L), or TAK-701 (50 μg/mL), as indicated. Cell lysates were then prepared and subjected to immunoblot analysis with antibodies to phosphorylated or total forms of EGFR, MET, AKT, or ERK, or with those to β-actin.

resistance in HCC827-HGF1 and -HGF2 cells as well as in HCC827 GR5 cells.

TAK-701 abrogates gefitinib resistance induced by HGF

To investigate the roles of MET and HGF in gefitinib resistance in HCC827 GR5 as well as in HCC827-HGF1 and -HGF2 cells, we exposed the cells to the MET-TKI PHA-665752 or to TAK-701, a humanized monoclonal antibody to HGF, in combination with gefitinib. Combined treatment with PHA-665752 and gefitinib was previously shown to result in substantial growth inhibition in HCC827 GR5 (*MET* amplification–positive) cells (6). We found that the combination of gefitinib and TAK-701 did not affect the growth of HCC827 GR5 cells (Fig. 3A). In HCC827-HGF1 and -HGF2 cells, however, TAK-701 and PHA-665752 each restored the sensitivity of cell growth to inhibition by gefitinib (Fig. 3B and C).

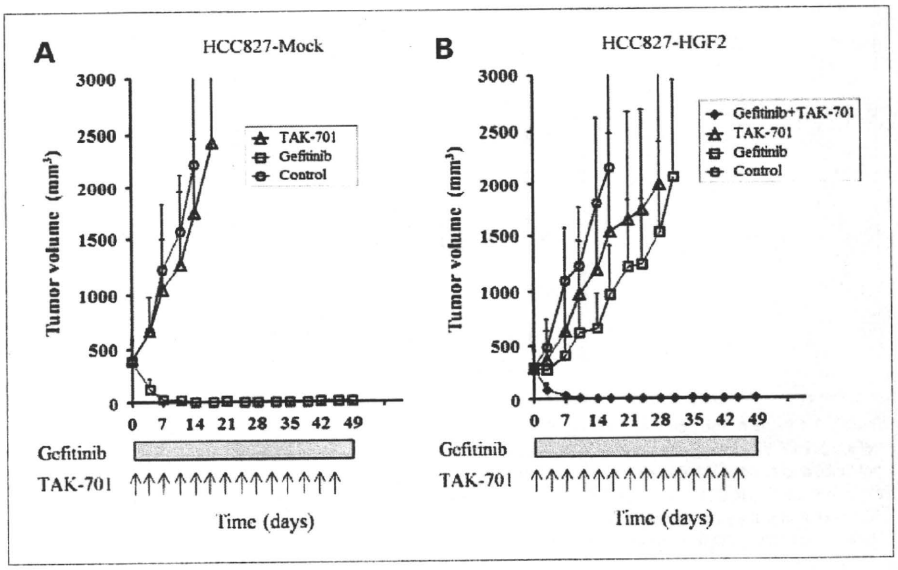

Figure 5. Effects of the combination of TAK-701 and gefitinib on the growth of gefitinib-resistant NSCLC cells *in vivo*. Nude mice with tumor xenografts established by s.c. injection of HCC827-Mock (A) or HCC827-HGF2 (B) cells were treated for 7 weeks with vehicle (control), gefitinib (50 mg/kg), TAK-701 (5 mg/kg), or both drugs, as described in Materials and Methods. Tumor volume was determined at the indicated times after the onset of treatment. Data are means ± SE from five mice per group. $P < 0.001$ for comparison of gefitinib versus gefitinib plus TAK-701 in B.

In addition, staining with Annexin V revealed that gefitinib alone induced a marked increase in the frequency of apoptosis in HCC827-Mock cells but elicited a much smaller effect in HCC827-HGF2 cells (Fig. 3D). However, treatment with both gefitinib and TAK-701 triggered an increase in the number of Annexin V–positive HCC827-HGF2 cells similar in extent to that induced by gefitinib alone in HCC827-Mock cells. These results thus indicate that TAK-701 restores gefitinib-induced apoptosis in HCC827-HGF2 cells.

To examine the effects of gefitinib, PHA-665752, and TAK-701 on cell signaling in the parental, HCC827 GR5, and HCC827-HGF2 cell lines, we again did immunoblot analysis (Fig. 4). Consistent with previous observations (6), PHA-665752 in combination with gefitinib inhibited MET, AKT, and ERK phosphorylation in HCC827 GR5 cells. We further found that TAK-701 alone did not inhibit MET phosphorylation, and thus the combination of TAK-701 and gefitinib did not abrogate AKT and ERK phosphorylation in HCC827 GR5 cells. In HCC827-HGF2 cells, however, TAK-701 as well as PHA-665752 inhibited MET phosphorylation, and the combined treatment with TAK-701 and gefitinib fully suppressed ERK and AKT phosphorylation. These results indicate that HGF-induced gefitinib resistance is mediated by HGF-MET signaling and is abrogated by treatment with TAK-701 in HCC827-HGF cells.

Cell-derived HGF induces gefitinib resistance in NSCLC cells and TAK-701 restores the sensitivity of tumor growth to inhibition by gefitinib *in vivo*

To examine the possible induction of gefitinib resistance by tumor cell–derived HGF and the efficacy of combined treatment with TAK-701 and gefitinib *in vivo*, we generated xenografts in nude mice by injection of HCC827-Mock or HCC827-HGF2 cells. We found that, whereas gefitinib markedly inhibited the growth of HCC827-Mock xenografts (Fig. 5A), HCC827-HGF2 xenografts were substantially resistant to gefitinib (Fig. 5B). TAK-701 alone had a minimal effect on tumor growth in both HCC827-Mock and HCC827-HGF2 xenograft models. However, the combination of gefitinib and TAK-701 induced marked regression of HCC827-HGF2 xenografts. These results thus suggest that HGF produced by NSCLC tumors harboring an *EGFR* mutation induces gefitinib resistance, and that TAK-701 abrogates such HGF-induced gefitinib resistance *in vivo*.

Discussion

In the present study, we established HGF-overexpressing sublines of HCC827 cells and showed that these sublines are resistant to gefitinib both *in vitro* and *in vivo*. To investigate whether the resistance of HCC827-HGF cells to gefitinib is attributable to HGF-MET signaling, we examined the effects of the MET-TKI PHA-665752 and of TAK-701, a humanized monoclonal antibody to HGF, on signal transduction and cell growth. In both HCC827-HGF1 and -HGF2 cells as well as in HCC827 GR5 cells, which are positive for *MET* amplification, gefitinib alone did not inhibit AKT or ERK phosphorylation, whereas gefitinib in combination with PHA-665752 markedly suppressed the phosphorylation of these signaling molecules. Consistent with these results, PHA-665752 restored the sensitivity of cell growth to inhibition by gefitinib in HCC827-HGF cells as well as in HCC827 GR5 cells. These results indicate that the gefitinib resistance of these cell lines is mediated by MET signaling. TAK-701 has been shown to potently inhibit HGF binding to MET in cancer cells and xenograft models dependent on autocrine HGF-MET signaling.[6] TAK-701 did not inhibit the phosphorylation of MET in HCC827 GR5 cells, suggesting that the activation of MET in these cells is not dependent on HGF. Indeed, we were not able to detect the secretion of HGF from HCC827 GR5 cells. In contrast, TAK-701 suppressed MET phosphorylation, and thus the combination of TAK-701 and gefitinib markedly inhibited both AKT and ERK signaling in HCC827-HGF cells, resulting in their growth inhibition. These results indicate that autocrine HGF-MET signaling contributes to gefitinib resistance in HCC827-HGF cells. Similar ligand-mediated gefitinib resistance has been described previously, with insulin-like growth factor having been found to rescue cells expressing wild-type *EGFR* from gefitinib-induced inhibition of cell growth (23). These observations suggest that ligand-dependent receptor tyrosine kinase (RTK) activation (by HGF or insulin-like growth factor), as well as ligand-independent RTK activation (by *MET* amplification), plays a pivotal role in the development of resistance to gefitinib. Further studies should reveal whether other ligand-RTK combinations contribute to gefitinib resistance.

We found that the baseline levels of both MET expression and MET phosphorylation in HCC827-HGF cells were lower than those in HCC827 GR5 cells (Fig. 2C), whereas HCC827-HGF cells were resistant to gefitinib to the same extent as HCC827 GR5 cells *in vitro* (Fig. 2B). These results suggest that phosphorylated MET activates downstream signaling through different pathways in HCC827 GR5 and HCC827-HGF cells. MET was recently shown to signal through ERBB3 in *MET* amplification–positive NSCLC cells (6) or through Grb2-associated binder 1 (Gab1) in NSCLC cells with HGF-induced gefitinib resistance (24). Further studies are required to investigate whether the biological properties of NSCLC cells or the abilities of drugs to overcome gefitinib resistance are affected by differences in RTK downstream signaling.

In our HCC827-HGF xenograft model, we showed that HGF secreted from *EGFR* mutation–positive NSCLC cells drives tumor growth even in the presence of gefitinib, and that combination therapy with TAK-701 and gefitinib was

[6] Kitahara O, Nishizawa S, Ito Y, Toyoda Y, Misumi Y, Sato S, Inaoka T, Klakamp SL, Kokubo T, Hori A. TAK-701, a humanized monoclonal antibody to human hepatocyte growth factor, exhibits promising antitumor effects on multiple tumor types. In preparation.

able to greatly inhibit the growth of HCC827-HGF tumors. These results indicate that interruption of HGF-MET signaling with TAK-701 represents a powerful strategy to abrogate gefitinib resistance induced by HGF derived from tumor cells. HGF was previously shown to be expressed predominantly by adenocarcinoma cells in NSCLC specimens, although a low level of HGF staining was also apparent in stromal cells (25). Furthermore, marked expression of HGF has been detected in most lung cancers with intrinsic or acquired resistance to gefitinib (10, 26). These data suggest that our autocrine model systems based on stable overexpression of HGF are clinically relevant and should prove useful for the establishment of strategies to overcome gefitinib resistance. HGF is also produced by stromal cells of various tumor types (13, 27, 28). Indeed, HGF derived from fibroblasts injected into nude mice together with *EGFR* mutation–positive NSCLC cells induced gefitinib resistance in the NSCLC cells *in vivo* (29). Further studies are required to clarify the major source of HGF that contributes to gefitinib resistance in patients with *EGFR* mutation–positive lung cancer. Given that TAK-701 inhibits HGF binding to MET, TAK-701 may reverse gefitinib resistance induced by HGF derived not only from tumor cells but also from stromal cells.

In conclusion, we have shown that autocrine activation of MET by HGF confers resistance to gefitinib, and that TAK-701, a humanized monoclonal antibody to HGF, restored sensitivity to gefitinib in tumors with HGF-induced gefitinib resistance. TKIs inhibit several signaling pathways and are therefore associated with a risk of high toxicity, whereas therapeutic antibodies are thought to be less toxic as a result of their high specificity. TAK-701 is currently undergoing phase I trials as a single agent in patients with advanced solid tumors, and our results now suggest that further studies of combination therapy with TAK-701 and gefitinib are warranted in NSCLC patients with HGF-induced EGFR-TKI resistance.

Disclosure of Potential Conflicts of Interest

No potential conflicts of interest were disclosed.

Grant Support

National Institute of Health R01CA135257 (P.A. Jänne) and National Cancer Institute Lung SPORE P50CA090578 (P.A. Jänne).

The costs of publication of this article were defrayed in part by the payment of page charges. This article must therefore be hereby marked *advertisement* in accordance with 18 U.S.C. Section 1734 solely to indicate this fact.

Received 05/25/2010; revised 08/09/2010; accepted 08/11/2010; published OnlineFirst 08/17/2010.

References

1. Lynch TJ, Bell DW, Sordella R, et al. Activating mutations in the epidermal growth factor receptor underlying responsiveness of non-small-cell lung cancer to gefitinib. N Engl J Med 2004;350:2129–39.
2. Paez JG, Janne PA, Lee JC, et al. EGFR mutations in lung cancer: correlation with clinical response to gefitinib therapy. Science 2004;304:1497–500.
3. Pao W, Miller V, Zakowski M, et al. EGF receptor gene mutations are common in lung cancers from "never smokers" and are associated with sensitivity of tumors to gefitinib and erlotinib. Proc Natl Acad Sci U S A 2004;101:13306–11.
4. Kobayashi S, Boggon TJ, Dayaram T, et al. EGFR mutation and resistance of non-small-cell lung cancer to gefitinib. N Engl J Med 2005;352:786–92.
5. Pao W, Miller VA, Politi KA, et al. Acquired resistance of lung adenocarcinomas to gefitinib or erlotinib is associated with a second mutation in the EGFR kinase domain. PLoS Med 2005;2:e73.
6. Engelman JA, Zejnullahu K, Mitsudomi T, et al. MET amplification leads to gefitinib resistance in lung cancer by activating ERBB3 signaling. Science 2007;316:1039–43.
7. Bean J, Brennan C, Shih JY, et al. MET amplification occurs with or without T790M mutations in EGFR mutant lung tumors with acquired resistance to gefitinib or erlotinib. Proc Natl Acad Sci U S A 2007;104:20932–7.
8. Bottaro DP, Rubin JS, Faletto DL, et al. Identification of the hepatocyte growth factor receptor as the c-met proto-oncogene product. Science 1991;251:802–4.
9. Naldini L, Vigna E, Narsimhan RP, et al. Hepatocyte growth factor (HGF) stimulates the tyrosine kinase activity of the receptor encoded by the proto-oncogene c-MET. Oncogene 1991;6:501–4.
10. Yano S, Wang W, Li Q, et al. Hepatocyte growth factor induces gefitinib resistance of lung adenocarcinoma with epidermal growth factor receptor-activating mutations. Cancer Res 2008;68:9479–87.
11. Nakamura T, Nishizawa T, Hagiya M, et al. Molecular cloning and expression of human hepatocyte growth factor. Nature 1989;342:440–3.
12. Maulik G, Shrikhande A, Kijima T, Ma PC, Morrison PT, Salgia R. Role of the hepatocyte growth factor receptor, c-Met, in oncogenesis and potential for therapeutic inhibition. Cytokine Growth Factor Rev 2002;13:41–59.
13. Birchmeier C, Birchmeier W, Gherardi E, Vande Woude GF. Met, metastasis, motility and more. Nat Rev Mol Cell Biol 2003;4:915–25.
14. Harvey P, Warn A, Newman P, Perry LJ, Ball RY, Warn RM. Immunoreactivity for hepatocyte growth factor/scatter factor and its receptor, met, in human lung carcinomas and malignant mesotheliomas. J Pathol 1996;180:389–94.
15. Tuck AB, Park M, Sterns EE, Boag A, Elliott BE. Coexpression of hepatocyte growth factor and receptor (Met) in human breast carcinoma. Am J Pathol 1996;148:225–32.
16. Koochekpour S, Jeffers M, Rulong S, et al. Met and hepatocyte growth factor/scatter factor expression in human gliomas. Cancer Res 1997;57:5391–8.
17. Danilkovitch-Miagkova A, Zbar B. Dysregulation of Met receptor tyrosine kinase activity in invasive tumors. J Clin Invest 2002;109:863–7.
18. Tsao MS, Zhu H, Giaid A, Viallet J, Nakamura T, Park M. Hepatocyte growth factor/scatter factor is an autocrine factor for human normal bronchial epithelial and lung carcinoma cells. Cell Growth Differ 1993;4:571–9.
19. Okabe T, Okamoto I, Tamura K, et al. Differential constitutive activation of the epidermal growth factor receptor in non-small cell lung cancer cells bearing EGFR gene mutation and amplification. Cancer Res 2007;67:2046–53.
20. Okamoto W, Okamoto I, Yoshida T, et al. Identification of c-Src as a potential therapeutic target for gastric cancer and of MET activation as a cause of resistance to c-Src inhibition. Mol Cancer Ther 2010;9:1188–97.